Reef fish functional groups show variable declines due to deforestation-driven sedimentation, while flexible harvesting mitigates this damage

Russell Milne[1,2,*,†], Madhur Anand[1,2], Chris T. Bauch[1,2]

1 Department of Applied Mathematics, University of Waterloo, Waterloo, Ontario, Canada
2 School of Environmental Sciences, University of Guelph, Guelph, Ontario, Canada

* Corresponding author. Email address: rmilne@ualberta.ca
† Current address: Department of Mathematical and Statistical Sciences, University of Alberta, Edmonton, Alberta, Canada

Abstract

Sedimentation is a major coral reef stressor, with effects including suppressing algae consumption by herbivorous fish. This puts pressure on reef fish populations and the fisheries that harvest them. Deforestation causes much sedimentation on reefs, and is an ongoing concern in Pacific island states. Although ecosystem processes like deforestation and fish population dynamics are usually far from equilibrium, explicitly time-dependent analyses of reef fish vulnerability to deforestation are rare. Additionally, optimization methods for fisheries on heavily sedimented reefs are generally unexplored. Here, we construct a model coupling four reef fish functional groups with seabed dynamics and deforestation, fit using data for the Solomon Islands. We show that with predicted human population increases, highland deforestation could cause herbivorous and omnivorous fish abundances to halve within 15-30 years, but that piscivorous fish and top predators are resilient to lowland deforestation. We demonstrate that flexible fishing approaches could lead to high and temporally stable populations of herbivorous fish and top predators, offsetting sedimentation-related stress. We show that the combination of deforestation and increased fishing demand due to human population growth may cause medium-term local reef fish extirpation. Our results provide sustainability guidelines for reef fisheries, and demonstrate nonlinear interactions between overfishing and deforestation.

Keywords

Coral reef fisheries; food web model; Solomon Islands; fishing quotas; soil erosion

Introduction

Sedimentation is projected to be a serious cause of coral reef degradation in the future [1, 2, 3], affecting many reef fish taxa [4]. Much of the sediment exported onto reefs is produced either directly or indirectly by deforestation [5], and deforestation itself has been mentioned as a threat to reef fish [6]. Hence, local forest overexploitation could lead to substantial declines in fish populations on adjacent reefs. However, this pressure could potentially be heterogeneous across fish functional groups, and the timing of when different functional groups can be expected to decline following deforestation is still relatively unexplored. As many coastal communities depend on reef fisheries for food [7], deforestation's effects could additionally include a collapse in fish catch. Therefore, optimization of fishing strategies on reefs with heavy sedimentation is a pressing concern.

Sediment washed onto reefs comes in large part from soil erosion [8], and cleared land tends to have significantly higher rates of erosion compared to forests [9, 10]. Hence, deforestation has been identified as a major cause of reef sedimentation [5]. When algal turf on the seabed becomes laden with sediment, it undergoes a qualitative shift to a form that is less productive and less palatable to herbivorous fish [3, 11], known as "long sediment-laden algal turf" (LSAT). This suppresses herbivory on the algal turf: for instance, herbivorous fish with scraping teeth avoid LSAT because they would have to ingest sediment with low nutritional value when they scrape algae off the seabed. This can lower herbivorous fish numbers [11], as herbivorous reef fish are particularly susceptible to bottom-up control [12]. Hence, through land-sea linkages, deforestation has the potential to severely impact reef fish populations. Because of these long-range effects, "ridge-to-reef" models have recently begun to be developed, in order to predict how forest clearance and other terrestrial drivers will affect future health of coral reefs (see e.g. [13, 14]).

Many existing ridge-to-reef models are static, offering a snapshot in time of what conditions on reefs may be like under different deforestation and management scenarios. However, linking deforestation to the health of coral and fish communities involves considering many interwoven processes, which may happen on different timescales [15, 16] and will often not be at equilibrium. For instance, deforestation may not happen at a constant rate [17], as the demand for cleared land or forest products that underpins it may vary. Similarly, marine fish taxa can be categorized based on factors such as lifespan and reproductive rates [18] that have clear implications for population growth. These life history differences affect susceptibility to different stressors: slow-growing, long-lived species are particularly vulnerable to rapid depletion due to overharvesting [19], while species with more rapid life history timescales may be more affected by increases in ocean temperature [20]. Relatedly, as food webs often contain complex patterns of interspecies links [21], cascading effects stemming from pressure on one given species could be felt at different times by other species that interact with it. Thus, in addition to anticipating future reef conditions, management plans must understand how quickly and in which order the events that lead to them take place.

Deforestation has been identified as a significant environmental concern in the West Pacific and Southeast Asia in recent decades [17, 22]. This includes the Solomon Islands, where logging has been estimated at seven times the sustainable yield [23]. Hence, concerns have been raised about forest loss on several of that country's constituent islands, such as Guadalcanal [24], Kolombangara [25, 10], and Rennell [26]. Of particular concern is logging on steep slopes and in highland areas, such as those found in the interior of Kolombangara [10], which has been described as a pervasive problem in the Solomon Islands [27, 28]. This is because erosion (and therefore sediment generation) can happen at a greater magnitude on such terrain [29, 30], particularly in areas where logging or other human disturbances take place [31, 32]. However, past deforestation on the Solomon Islands has

been spatially uneven, and many areas still have close to complete forest cover [23, 33]. Therefore, it is important to establish expectations for how large-scale deforestation in these areas could affect local reef fish populations before it happens.

Human activity can significantly negatively impact reef fish assemblages [34]. Sedimentation from offshore construction can change community composition on a coral reef over a long timescale [35], and clear-cutting mangroves can alter fish assemblages [36] by harming species that use mangroves as nurseries. Similar effects have been found in riparian habitats, where deforestation along the banks of streams reduces fish niche diversity [37] and drives shifts to more sediment-tolerant species [38, 39]. Recent studies have begun to examine how sedimentation due to inland deforestation affects the populations of different reef fish taxa [13, 14], although this work has mostly covered different groupings of herbivorous fish rather than fish elsewhere in a coral reef food web. Therefore, ridge-to-reef models could be further used to predict population changes of many different reef fish functional groups, to holistically evaluate fish assemblage changes.

Coral reef fisheries represent a significant food source in tropical island states [7]. However, many such countries, among them the Solomon Islands, will experience substantial human population growth in the next few decades [40], which will put pressure on local fish populations. The intuitive result that more population means greater demand for fish has been observed as both increasing fishing effort over time in growing areas [41] and a correlation between population density and fishing effort [42]. Additional deforestation may accompany these fishing rate increases: empirical relationships between an area's population and its forest cover have been obtained in many different parts of the world [43, 44, 45]. Previous studies on multiple coral reef stressors have found that overfishing and sedimentation can have significant interaction effects [46, 47]. This suggests that via deforestation's effects on sedimentation, overharvesting of one resource (forest) can potentially also lead to shortages in another one (reef fish). Hence, the maintenance of fisheries after shifts to heavily sedimented conditions has been mentioned as a priority for research [11].

Here, we construct a land-sea model featuring deforestation and sedimentation, parametrized for the Solomon Islands. We use this model to investigate the time-dependent responses of different fish functional groups to deforestation-driven sedimentation, and how this could affect the productivity of reef fisheries.

Methods

Model building

To model how deforestation and the sediment buildup associated with it could affect reef fish populations and the viability of harvesting them, we adapted a model of Fung *et al.* [48]. We chose this model because it includes a compartment for turf algae, which we use when investigating fishing potential on algal turf-dominated reefs, and because the authors estimated how sedimentation affected their model parameters within their original derivations. This model features state transitions between coral C, turf algae T, macroalgae M, and open space Q on a seabed; as the total seabed area is constant, space is defined as $Q = 1 - C - T - M$. In [48], C, T, M, and Q represent average benthic cover across a relatively homogeneous reef area, with a spatial scale on the order of 10^1 to 10^3 m. The original equations in [48], which we retained, are below:

$$\begin{aligned}
\frac{\mathrm{d}C}{\mathrm{d}t} &= \left(l_{C}^{s} + l_{C}^{b}C\right)\left(Q + \varepsilon_{C}T\right) + r_{C}\left(1 - \beta_{M}M\right)\left(Q + \alpha_{C}T\right)C - d_{C}C - \gamma_{MC}r_{M}MC \\
\frac{\mathrm{d}T}{\mathrm{d}t} &= \zeta_{T}\left(1 - \theta\right)Q - g_{T}\theta T - \varepsilon_{C}\left(l_{C}^{s} + l_{C}^{b}C\right)T - \alpha_{C}r_{C}\left(1 - \beta_{M}M\right)TC - \gamma_{MT}r_{M}MT \\
\frac{\mathrm{d}M}{\mathrm{d}t} &= r_{M}M\left(Q + \gamma_{MC}C + \gamma_{MT}T\right) - g_{M}\theta M
\end{aligned} \tag{1}$$

Here, coral larvae are produced by local brooding corals at a rate l_{C}^{b}, and by exogenous spawning corals at a rate l_{C}^{s}. These larvae can settle on open space or algal turf, with ε_{C} being the relative rate at which coral larvae settle on turf relative to open space. Coral also laterally expands at a baseline rate r_{C}, with α_{C} being the relative rate at which coral expands into algal turf compared to open space (analogous to ε_{C}). Coral lateral expansion is suppressed by macroalgae according to a factor β_{M}. Coral dies at a rate d_{C}, after which the space it takes up reverts to being empty. Algal turf expands over space at a rate ζ_{T}, which is scaled down according to a unitless quantity θ between 0 and 1 representing grazing pressure; existing algal turf is also cleared by grazing at a rate $g_{T}\theta$, where g_{T} is the maximum rate at which turf is grazed. Macroalgae has an intrinsic rate of growth r_{M}, and is grazed at a rate $g_{M}\theta$, where g_{M} is the maximum yearly rate that macroalgae is removed due to grazing. Macroalgae expands over coral and turf according to the relative rates γ_{MC} and γ_{MT}, respectively, which are normalized according to its rate of expansion into open space (as with ε_{C} and α_{C}). Because we expanded this model to explicitly include herbivory and sedimentation, we took θ, r_{C}, l_{C}^{b}, l_{C}^{s}, and d_{C} to vary rather than being constant (see below). All other model features were kept identical to those in [48].

To this model, we added four different fish functional groups: herbivores (e.g. *Scarus dimidiatus*), omnivores (e.g. *Acanthurus triostegus*), piscivores (e.g. *Epinephelus merra*), and top predators (e.g. *Sphyraena forsteri*). These were assumed to follow logistic growth, with intrinsic growth rates of r_{H}, r_{O}, r_{P}, and r_{Z}, respectively, and carrying capacities of 1. Each functional group's growth rate was further scaled according to food availability. Herbivorous fish were assumed to only eat algae. Since herbivory is suppressed by accumulation of algal turf sediment [49, 50], we introduced a quantity $\mu(t)$ representing this decrease (see below). Omnivorous fish had an assumed diet consisting partly of algae, at proportion δ_{O}, and partially of alternative food sources such as zooplankton, at proportion $1 - \delta_{O}$. The availability of zooplankton was in turn modelled using a function $\phi(t)$; see below. The diet of piscivorous fish was assumed to consist of herbivorous and omnivorous fish in proportions δ_{P} and $1 - \delta_{P}$, respectively; top predators were assumed to eat herbivorous, omnivorous, and piscivorous fish in proportions δ_{Z}^{H}, δ_{Z}^{O}, and $1 - \delta_{Z}^{H} - \delta_{Z}^{O}$, respectively. Fish were assumed to be harvested at rates h_{H}, h_{O}, h_{P}, and h_{Z}. All fish functional groups aside from top predators were assumed to die from predation at rates m_{H}, m_{O}, and m_{P}; these were scaled according to the abundance of each functional group's predators. As with the benthos, we assumed spatially relatively homogeneous fish populations; dispersal-induced population dynamics (e.g. [51]) were therefore folded into local averages. The differential equations for fish populations are below:

$$
\begin{aligned}
\frac{\mathrm{d}F_{H}}{\mathrm{d}t} &= \frac{r_{H}}{1+\mu}F_{H}\left(1-F_{H}\right)\left(T+\frac{g_{M}}{g_{T}}M\right)-h_{H}F_{H}-m_{H}F_{H}\frac{\delta_{P}F_{P}+\delta_{Z}^{H}F_{Z}}{\delta_{P}+\delta_{Z}^{H}}\\
\frac{\mathrm{d}F_{O}}{\mathrm{d}t} &= r_{O}F_{O}\left(1-F_{O}\right)\left(\frac{\delta_{O}}{1+\mu}\left(T+\frac{g_{M}}{g_{T}}M\right)+\left(1-\delta_{O}\right)\phi\right)-h_{O}F_{O}-m_{O}F_{O}\frac{\left(1-\delta_{P}\right)F_{P}+\delta_{Z}^{O}F_{Z}}{1-\delta_{P}+\delta_{Z}^{O}}\\
\frac{\mathrm{d}F_{P}}{\mathrm{d}t} &= r_{P}F_{P}\left(1-F_{P}\right)\left(\delta_{P}F_{H}+\left(1-\delta_{P}\right)F_{O}\right)-h_{P}F_{P}-m_{P}F_{P}F_{Z}\\
\frac{\mathrm{d}F_{Z}}{\mathrm{d}t} &= r_{Z}F_{Z}\left(1-F_{Z}\right)\left(\delta_{Z}^{H}F_{H}+\delta_{Z}^{O}F_{O}+\left(1-\delta_{Z}^{H}-\delta_{Z}^{O}\right)F_{P}\right)-h_{Z}F_{Z}
\end{aligned}
\tag{2}
$$

To investigate the effects of deforestation and sedimentation on reef fish populations, we added three more model components: forest cover in land areas adjacent to the reef, concentration of suspended sediment within the water column on the reef, and amount of sediment that has accumulated on the seabed. We represented these using the variables X (a percentage), S_{W} (measured in mg cm^{-3}), and S_{B} (a dimensionless constant), respectively. A schematic of the full model can be seen in Figure 1. Our differential equation for forest cover contained a deforestation term and a forest regrowth term. The deforestation term was based on the relationship between forest cover X and population size N (i.e. $\frac{\mathrm{d}X}{\mathrm{d}N}$) from a data-driven model by Tanaka *et al.* [43], as well as a time-varying rate of population growth (i.e. $\frac{\mathrm{d}N}{\mathrm{d}t}$) sourced from United Nations projections [40]; this term featured a baseline deforestation rate of r_{X}. (Note that N is scaled by present-day population.) The forest regrowth term was logistic, with a baseline regrowth rate of a_{X}. Suspended sediment was modelled as arriving on the reef via river outflow. We assumed that sediment concentration in local rivers scales linearly with local forest cover [9, 10], taking values of q_{b} at 100% forest cover and $q_{b}+q_{c}$ at 0%, and that this river sediment reaches the reef at a rate λ. Suspended sediment was assumed to be exported out of the reef at a rate e. We expressed sediment on the seabed S_{B} as a ratio between the level at a given time and a level corresponding to pristine conditions, under the assumption that S_{B} would be in equilibrium with S_{W}. The forest and sediment equations are below:

$$
\begin{aligned}
\frac{\mathrm{d}X}{\mathrm{d}t} &= \frac{\mathrm{d}X}{\mathrm{d}N}\frac{\mathrm{d}N}{\mathrm{d}t}+a_{X}X(1-X)=-r_{X}NX\frac{\mathrm{d}N}{\mathrm{d}t}+a_{X}X(1-X)\\
\frac{\mathrm{d}S_{W}}{\mathrm{d}t} &= \left(q_{b}+\left(1-X\right)q_{c}\right)\lambda-eS_{W}\\
S_{B}\left(t\right) &= \frac{S_{W}\left(t\right)}{S_{W}\left(t=0\right)}
\end{aligned}
\tag{3}
$$

Our differential equations feature several time-varying parameters. $\mu(t)$ represents the degree to which seabed sediment suppresses herbivory, which logarithmically increases with S_{B}. $\theta(t)$ is the grazing pressure on algae, which has a baseline rate of $\tilde{\theta}$, can be scaled down by μ, and depends on the abundances of fish functional groups that have algae in their diet. Coral lateral growth (r_{C}) and larval recruitment (l_{C}^{b} and l_{C}^{s}) decrease with the rate at which sediment accumulates on the seabed, while coral death (d_{C}) increases with it. We modelled these processes using baseline rates $\tilde{r}_{C}$, $\tilde{l}_{C}^{b}$, $\tilde{l}_{C}^{s}$, and $\tilde{d}_{C}$ scaled up or down according to the sedimentation rate r_{Sed}, with scaling constants κ_{r}, κ_{b}, κ_{s}, and κ_{d} governing these relationships. We took r_{Sed} itself to have a baseline rate of k_{Dep} and vary with F_{H}, since herbivorous fish can reduce sediment buildup by biting into it while feeding [52, 53]. Zooplankton dynamics happen over a faster timescale than the rest of the processes in

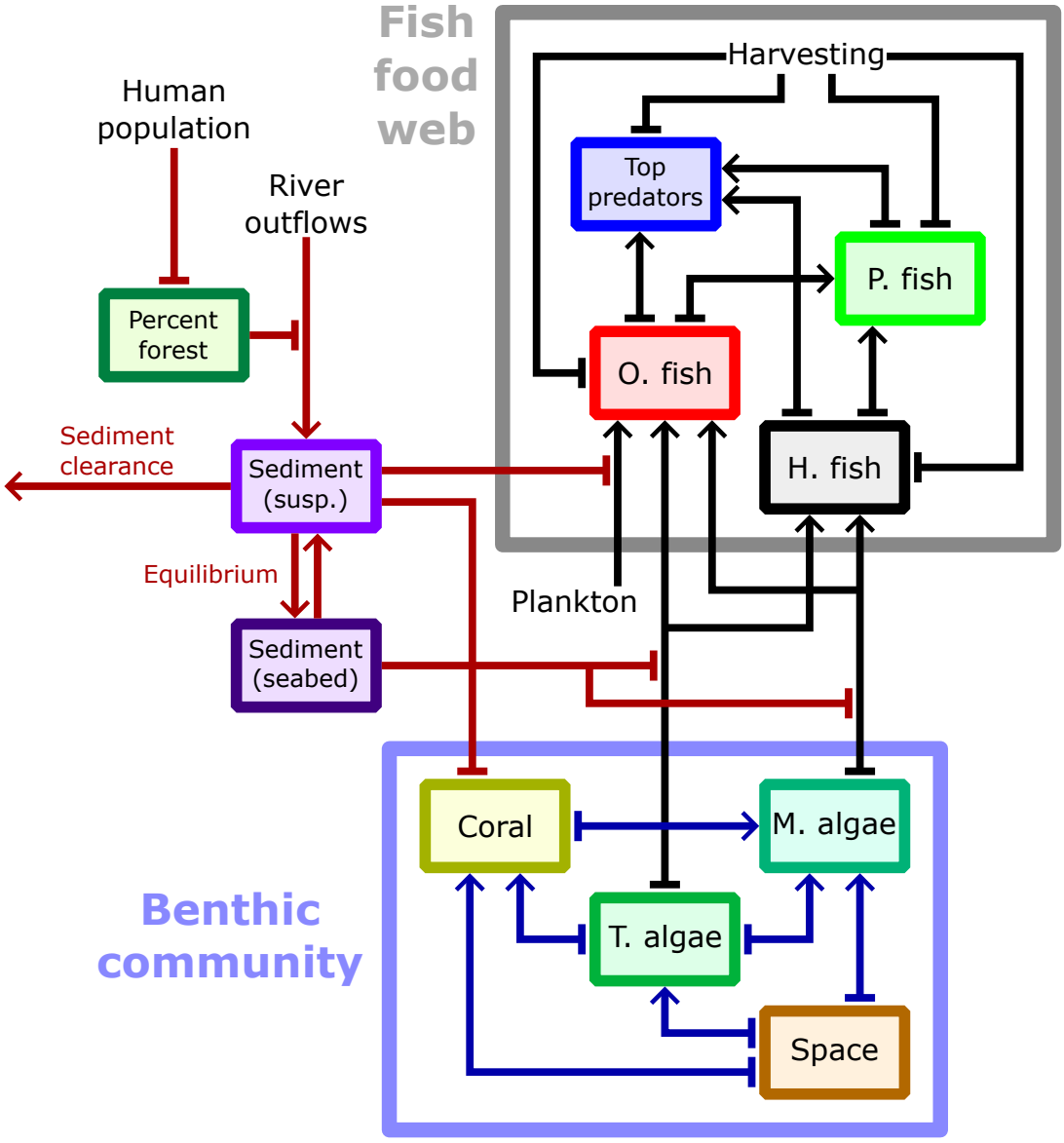

Figure 1: Diagram containing interactions in the model. Trophic interactions involving reef fish are shown in black, patterns of overgrowth on the benthos are shown in blue, and processes related to deforestation and sediment transport are shown in red. Pointed heads denote positive effects, while rectangular heads denote negative effects.

our model [54], and plankton population dynamics are less complex in more active waters [55] such as those near the mouth of a river. Hence, rather than model phytoplankton-zooplankton interactions directly, we considered zooplankton availability (ϕ) to decrease with sediment in the water column S_W according to the Lambert-Beer law of light attenuation, having it implicitly depend on phytoplankton photosynthesis. The time-varying functions mentioned here are below:

$$\begin{gathered}
\mu(t) = \max[\log_2(S_B), 0] \\
\theta(t) = \frac{\tilde{\theta}(F_H + \delta_O F_O)}{(1+\mu)(1+\delta_O)} \\
r_{\text{Sed}}(t) = \max[1 + (1 - 2F_H), 1]\, k_{\text{Dep}} S_W \\
r_C(t) = \frac{\tilde{r}_C \kappa_r}{\kappa_r + r_{\text{Sed}}}; \quad l_C^b(t) = \frac{\tilde{l}_C^b \kappa_b}{\kappa_b + r_{\text{Sed}}}; \quad l_C^s(t) = \frac{\tilde{l}_C^s \kappa_s}{\kappa_s + r_{\text{Sed}}} \\
d_C(t) = \tilde{d}_C \left(1 + \frac{r_{\text{Sed}}}{\kappa_d}\right) \\
\phi(t) = \exp\left(-\tilde{\phi} S_W\right)
\end{gathered} \tag{4}$$

Full derivations of all model functions are in Appendix A. Values of parameters related to fish growth, harvesting, and diet composition were scraped from the fish database FishBase [56]; all fish recorded by FishBase as living on Solomon Islands reefs with available data were assigned to a functional group based on their diet. Parameters taken from Fung *et al.* [48] were kept at the values in their model; other parameter values were chosen based on prior field studies, primarily ones on Solomon Islands coral reefs. A full account of the model parametrization, including Tables B.1 and B.2 containing all parameter values, is in Appendix B.

Simulation methods

To determine how fish assemblages in the Solomon Islands changed with deforestation, we simulated the population dynamics of each fish functional group while increasing the population of the Solomon Islands based on United Nations predictions starting in 2022 [40], for varying values of the forest loss constant r_X. We did this for $e = 0.1$, 0.5, and 0.9 to control for local variance in off-shelf sediment export, and $q_c = 0.043$ and 0.31 to represent lowland and highland deforestation. In each model run, initial conditions for each state variable were set to the steady state reached by that variable in the case where $X(t = 0) = 1$ and $r_X = 0$ (i.e. without deforestation), to simulate effects in a part of the Solomon Islands that currently has close to full forest cover (see e.g. [23, 33]). To isolate the decline in fish populations that was directly attributable to deforestation, we divided fish populations in each functional group at $t = 20$ and 50 years by the corresponding populations at $t = 20$ or $t = 50$ without deforestation. We also examined the sensitivity of medium-term fish decline in each functional group to local hydrological conditions, namely q_b and e. Further details on this are contained within Appendix D.

To evaluate the effectiveness of flexible harvesting strategies as a conservation tool in the face of sedimentation, we simulated fish populations for static and dynamic harvesting rates. Specifically, we derived harvesting rates for each functional group that solely depended on their relative proportions of the total fish population, denoted $h_{\text{Var},I}$, $h_{\text{Var},O}$, $h_{\text{Var},P}$, and $h_{\text{Var},Z}$; this derivation is explained in Appendix C. We subsequently constructed weighted averages of the baseline harvesting

rates for each functional group (e.g. h_H) and the rates that depend on current availability (e.g. $h_{\mathrm{Var},H}$), with a weighting constant k_h:

$$\bar{h}_I(t) = \frac{h_I + k_h h_{\mathrm{Var},I}}{1+k_h}, \quad I \in \{H, O, P, Z\} \tag{5}$$

We generated time series of fish populations for $k_h = 0$ (the baseline with static fishing rates obtained from FishBase), 0.1, 0.3, and 1 (50 percent dependence on local fish availability). These simulations were run under lowland deforestation conditions with all parameters at their baseline values in Tables B.1 and B.2. We also obtained the amount of time taken by each fish functional group to halve when affected by highland deforestation for $k_h = 0$ and 1, while varying values of r_X and e.

To test the robustness of reef fisheries to deforestation-driven sedimentation, as well as the persistence ability of reef fish, we simulated fish populations in a scenario where the amount of fish harvested was constant, i.e. with specified fishing quotas. We therefore derived harvesting rates corresponding to constant fishing quotas for each fish functional group; these derivations are in Appendix C. Our formulations for these rates included a scaling constant ρ representing the quota; $\rho = 1$ denoted a quota equal to the steady-state fish catch in the scenario without deforestation. Using these rates, we ran simulations for different values of ρ and r_X, for both lowland and highland deforestation scenarios. For each simulation, we obtained the amount of fish present at time $t = 50$. If this was zero, we additionally obtained the time of fish extinction. The constant-quota harvesting rates are as follows:

$$\bar{h}_I(t) = \rho F_I \frac{\left(h_H F_H(0) + h_O F_O(0) + h_P F_P(0) + h_Z F_Z(0)\right)}{F_H{}^2 + F_O{}^2 + F_P{}^2 + F_Z{}^2}, \quad I \in \{H, O, P, Z\} \tag{6}$$

To model rising demand for fish as population increases, we modified our baseline harvesting rate $h_I(t)$ for each functional group I by multiplying it by $1 + \nu N$, for a scaling constant ν. Under this assumption, we evaluated how deforestation and increased fishing rates jointly affect fish population size and fishing yield by running simulations for varying values of ν and r_X, and taking the population of all functional groups at time $t = 50$ years and the total number of fish harvested during each simulation. (For each functional group, the amount harvested was obtained by integrating that functional group's population times its harvesting rate.) This was done for both lowland and highland deforestation scenarios.

Results

Fish functional groups show differential resilience to deforestation-induced sedimentation

We found deforestation to have significant time-dependent effects on reef fish community composition: the functional groups most burdened by sedimentation differed in the medium-term and long-term (Figure 2). Generally, fish at lower trophic levels saw sharper declines first, while those at higher trophic levels were harmed more in the long run. After 20 years of lowland deforestation, herbivorous fish populations usually showed the largest decreases (Figure 2a). Higher off-shelf sediment export caused greater decline in herbivorous fish; this was reversed for the other functional groups, with omnivorous fish becoming the hardest-hit functional group when most sediment was

locally retained ($e = 0.1$). After 50 years of lowland deforestation, herbivorous fish populations usually decreased to 60-70 percent of their normal levels, with these declines unaffected by off-shelf sediment export rates (Figure 2b). Although lower values of e were associated with greater algal turf benthic cover, the high sediment load on this turf meant that the extra space taken up by it did not translate into higher long-term herbivorous fish populations. In contrast, the declines of the other three functional groups were heavily dependent on local sediment dynamics in this scenario. Under moderate to high deforestation, omnivorous fish populations ranged anywhere from 20 to 90 percent of what they would be with full forest cover, depending on e. Piscivorous fish and top predators maintained their numbers very well when sediment was mostly deposited away from reefs, but suffered comparable declines to herbivorous fish when $e = 0.1$.

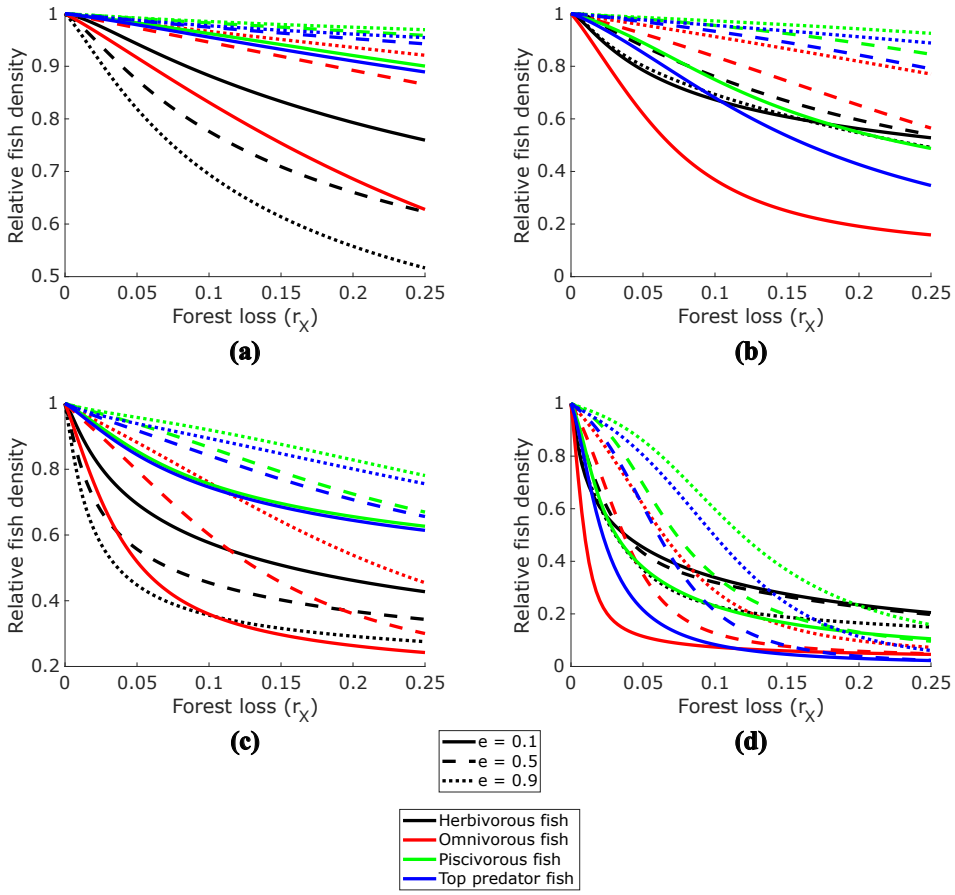

Figure 2: Abundances of fish functional groups after 20 years (Figure 2a) and 50 years (Figure 2b) of lowland deforestation, and 20 years (Figure 2c) and 50 years (Figure 2d) of deforestation on steep slopes, relative to the baseline case without deforestation. Note the difference in vertical axis scales.

Deforestation on steep slopes caused much greater declines in fish populations. After 20 years,

populations of herbivorous and omnivorous fish had halved in the median scenario (Figure 2c), with the same dependence on e as that seen with lowland deforestation. Following 50 years, all fish functional groups had experienced large and sometimes catastrophic declines (Figure 2d). For high $r_{_X}$ and low e (when large volumes of sediment were exported onto the simulated reef and retained there), populations of omnivorous fish and top predators could reach critically low levels, with local extinction probable soon after. Herbivorous fish showed the most long-term resilience, due to the total shift from coral to algal turf dominance providing them with a steady food source. However, since this algal turf was unpalatable LSAT, herbivorous fish populations were far below their pristine values, and too low to support any species at higher trophic levels.

Flexible harvesting strategies can stabilize fish populations on reefs with heavy sedimentation

Varying which fish were harvested depending on their availability while keeping the same overall harvesting rate caused very large population increases in two of the model's four functional groups (Figure 3). Herbivorous fish and top predators had about 60% and 50% higher populations after 50 years of lowland deforestation when $k_{_h} = 1$ (indicating a harvesting strategy 50% based on fish availability) compared to the baseline scenario without harvesting flexibility ($k_{_h} = 0$). The populations of omnivorous and piscivorous fish also increased with $k_{_h}$ to a lesser degree. Importantly, flexible harvesting also stabilized the populations of herbivorous fish and top predators: for $k_{_h} = 1$, the populations of these two functional groups were nearly constant after $t = 20$, at levels significantly above their initial values (Figures 3a, 3d). It also attenuated the decline of piscivorous fish, which had a population at $t = 50$ approximately equal to its initial value in the case where $k_{_h} = 1$, albeit with a decreasing trend (Figure 3c). In contrast, omnivorous fish saw few benefits from this strategy (Figure 3b), due to their high steady-state population without deforestation and low baseline harvesting rate.

Harvesting flexibility also provided substantial protection for most fish functional groups against the heavy sedimentation stress induced by highland deforestation (Figure 4). In the baseline highland deforestation scenario, all fish populations at least halved during our 50-year simulation window (Figure 4a). For herbivorous fish, this took as few as 10 years, depending on local conditions, and the populations of ordinarily robust functional groups (piscivorous fish and top predators) typically halved in 30 to 40 years. However, assuming a flexible harvesting program ($k_{_h} = 1$) meant that halving did not occur for herbivorous fish or top predators within 50 years, regardless of local hydrodynamic conditions, and it only occurred for piscivorous fish when deforestation was especially severe, i.e. $r_{_X} \gtrapprox 0.17$ (Figure 4b). For these three functional groups, flexible harvesting reduced highland deforestation's effects to a magnitude similar to what may be expected under deforestation on flatter lowland terrain. Omnivorous fish only saw mild benefits, with flexible harvesting delaying their halving by a few years.

Deforestation harms fisheries yield, and highland deforestation can cause it to collapse

We found that if harvesting rates start at their observed baseline values and increase with population growth, fish populations decline but total fish catch does not necessarily increase (Figure 5). Specifically, increasing the rate ν at which demand for fish rises with population growth usually did not lead to greater numbers of fish harvested (Figures 5c, 5d), due to fish becoming more depleted

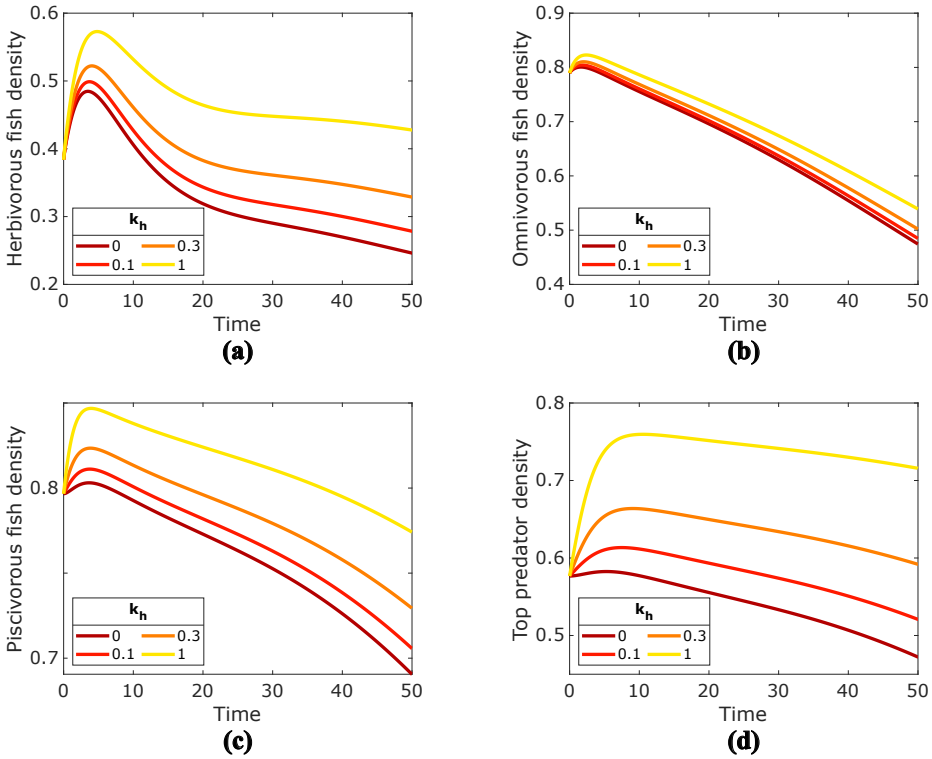

Figure 3: Populations of herbivorous fish (Figure 3a), omnivorous fish (Figure 3b), piscivorous fish (Figure 3c), and top predator fish (Figure 3d) for different values of the fishing flexibility constant k_h. Here, $e = 0.5$, $r_X = 0.23$, and $q_c = 0.043$.

under the lowland deforestation scenario (Figure 5a) and being locally extirpated under the highland deforestation scenario (Figure 5b). We additionally found that if population growth leads to increased demand for fish, 50 years of highland deforestation would result in fish populations going to zero even if relatively little forest is removed (Figure 5b).

Our results similarly show that if fish harvesting is done according to fixed quotas, harvesting levels that would normally be sustainable can instead cause local fish extirpation when deforestation is severe enough, particularly when it occurs on steep slopes (Figure 6). We found that if the raw number of fish harvested in the Solomon Islands did not deviate from current levels (i.e. $\rho = 1$), which were evaluated as being sustainable under present conditions, the increases in sedimentation brought on by highland deforestation would induce local fish extirpation by $t = 50$ under all but the most optimistic scenarios (Figures 6b, 6d). This occurred in as few as 25 years when deforestation happened at the same rate as was observed in Borneo in previous decades (Figure 6d). Less extreme effects were observed under lowland deforestation. Fish population declines were still evident in that scenario, and local extirpation was still possible for the highest values of r_X. However, under lowland deforestation, maintaining harvesting quotas at 80% of estimated current levels resulted in reasonably healthy fish populations at $t = 50$ even under the highest values of r_X tested.

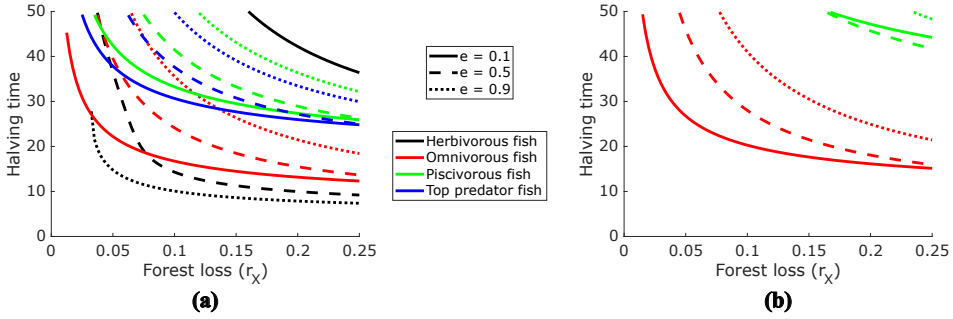

Figure 4: Time taken by fish functional groups to halve from their initial population sizes during highland deforestation, for different values of the forest loss constant r_x and the off-shelf sediment export rate e. Shown are the case where harvesting of all functional groups occurs at their baseline values (Figure 4a), and the case when harvesting partially depends on functional group availability with $k_h = 1$ (Figure 4b).

Discussion

Our results show that after 20 years of deforestation and its associated sedimentation, herbivorous fish were more abundant in areas with less off-shelf sediment export (Figure 2). We also found that herbivorous fish populations rose during the first 5-10 years of our deforestation simulations, peaking above their estimated pristine levels (Figure 3a). Both of these results point to coral being put under pressure from high sediment levels first, with herbivorous fish being more resilient. This result has parallels in previous field work done in the Solomon Islands, in which coral appeared to decline in health over a 5-year period following the onset of heavy sedimentation, but effects on fish abundance were less evident [28]. Similarly, observations at a site in Hawaii in 1976 and 1996 that had experienced intense sedimentation pressure due to offshore development showed a catastrophic decline in coral cover, but a mixture of decreasing and stable populations in reef fish [35]. These results support our findings that coral is more immediately susceptible to sedimentation and that twenty years of heavy sedimentation is enough time for some fish taxa to collapse.

Piscivorous fish and top predators were often resistant to deforestation's effects, although this was complicated by the possibility of bottom-up trophic cascades. Whenever herbivorous fish populations crashed to very low levels, this was followed by similar declines in piscivorous fish and top predators about 20 years later, but this effect was not seen when herbivorous fish populations were only reduced by moderate amounts (Figures 2, 4a). Additionally, in simulated areas where almost all sediment discharged from rivers is locally retained, we observed large declines in piscivorous fish and top predator populations approximately 15 years following declines in omnivorous fish, even though herbivorous fish were able to subsist on the massive amounts of low-quality algal turf (Figure 4a). This reduced the predation pressure on herbivorous fish, attenuating their decline even further. It is known that herbivorous reef fish are sensitive to bottom-up control [12], whereas our results show that this sensitivity may be lessened for fish at higher trophic levels.

Our results indicate three different regimes of fish population decline due to deforestation-driven sedimentation. In areas with naturally high turbidity, we expect omnivorous fish to collapse first, followed by species at higher trophic levels, with herbivorous fish showing milder declines. When deforestation either happens on highland terrain or at a fast rate, we expect herbivorous fish to

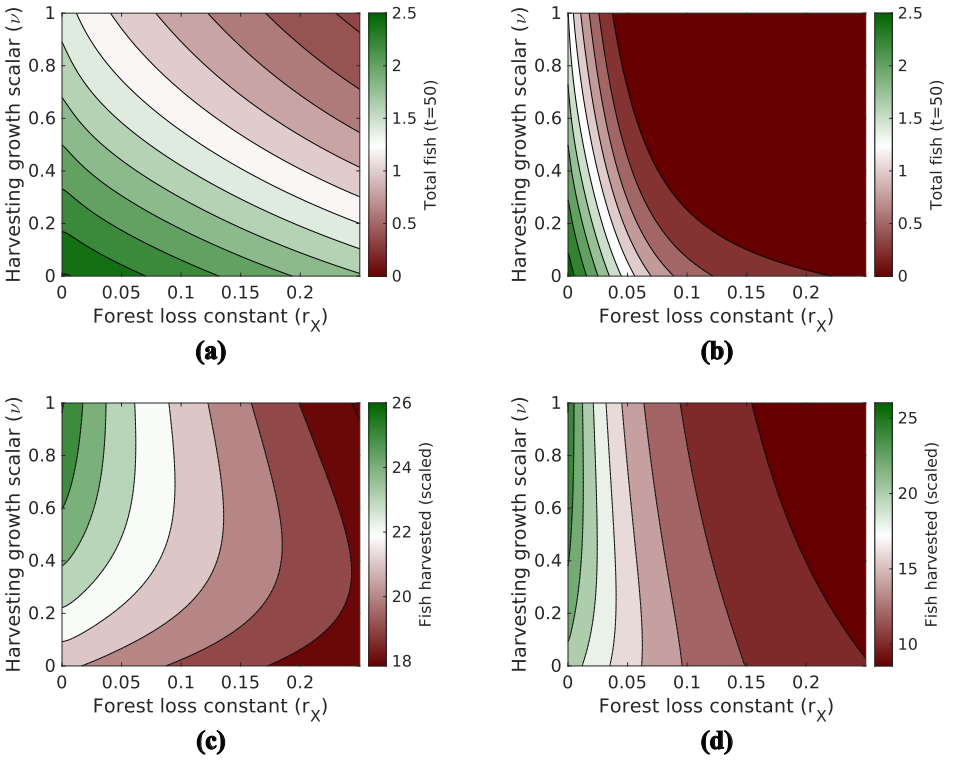

Figure 5: Fish populations from all functional groups after 50 years of deforestation (Figures 5a, 5b), as well as total fish harvested during that time (Figures 5c, 5d), when demand for fish increases with population growth. (Baseline harvesting rates are the constants shown in Table B.1, i.e. $k_h = 0$.) Figures 5a and 5c show the case with lowland deforestation, while Figures 5b and 5d show the case with highland deforestation.

be the first to drop to critical levels, followed by omnivorous fish 10 to 20 years later, then fish at higher trophic levels. When deforestation happens relatively slowly and on flat lowland terrain, we expect herbivorous fish to exhibit moderate declines, followed by omnivorous fish soon after, but piscivorous fish and top predators should maintain relatively high abundance. Under these conditions, if deforestation is contained in relatively small areas (e.g. $r_x \approx 0.05$, about one fourth of the deforestation rate seen in Borneo in the past few decades) and local waters are not naturally turbid, losses in fish abundance should be minimal.

Our findings on the resistance to sedimentation shown by fish at high trophic levels, as compared with herbivorous and omnivorous fish (Figures 2, D.1), are in concordance with a recent study on Western Australian reefs by Moustaka *et al.* [57]. This study showed that abundances of herbivorous scrapers and planktivorous omnivores had significant negative correlations with water turbidity, but generalist carnivores were substantially less affected by it. Our model provides a mechanistic framework for explaining these results, and can be used for testing their robustness in other locations due to the comprehensiveness of FishBase data [56].

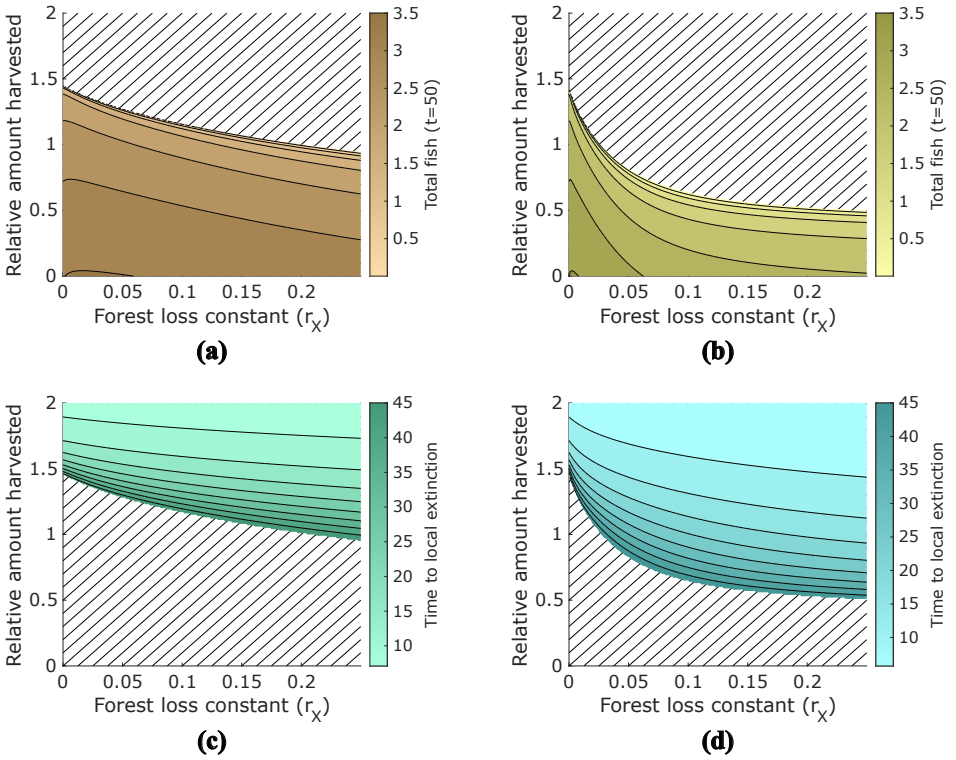

Figure 6: Robustness of reef fish and fisheries to changes caused by deforestation, assuming constant fishing quotas (specified by ρ, on the vertical axis). Figures 6a (lowland deforestation scenario) and 6b (highland deforestation scenario) show the amount of fish in all functional groups combined at $t = 50$, with diagonal hashing indicating that all fish populations were zero at this time. Figures 6c (lowland) and 6d (highland) show the time at which herbivorous fish became locally extinct in these cases, with diagonal hashing indicating that they did not go extinct.

Our simulations with both steadily increasing fishing pressure (Figure 5) and constant quota levels (Figure 6) show how interaction effects between overfishing and deforestation-driven sedimentation on reef fish abundance can change given local conditions. It has previously been shown that when nutrient levels are low, overfishing and sedimentation can have nonlinear masking effects on algal turf length (a proxy for turf quality), but for high nutrient levels this interaction becomes linear [46]. We considered similar interaction effects on quantities such as long-term fish population sizes, time to local extinction, and total catch over 50 years. For lowland deforestation, the interaction effects with fishing pressure were close to linear (Figures 5a, 6a, 6c), although nonlinearities were seen in the combined effects of lowland deforestation and growth in fish demand on fisheries yield (Figure 5c). However, exposure to both highland deforestation and high fishing rates produced compounding effects on fish local extinction risk (Figures 5b, 6b, 6d). This shows the potential for small increases in rates of deforestation or fish harvesting to have outsize impacts on reef fish persistence.

We found that flexible harvesting strategies allowed herbivorous fish and top predators to persist at reasonable levels even in the face of severe sedimentation pressure caused by highland deforestation (Figure 4b). Strategies such as our recommended ones can be implemented in a variety of ways. For instance, reef fisheries target different species by using different gear, such as beach seines, spearguns, fish traps, nets, and hand lines [58], although some overlaps exist. Fishing restrictions based on gear can therefore be used to redistribute, rather than reduce, a fishery's efforts [59], ideal for carrying out a strategy that keeps total fishing rate constant but varies which fish are targeted. Fishers have been more receptive to gear restrictions compared to the establishment of no-take areas [60], and management schemes' acceptance by local fishers is key for their success [61]. Such restrictions can also be dynamically updated based on field observations of which species need greater protection, which would greatly reduce risk from deforestation (see Figures 3 and 4).

The preferences of fishers have been previously noted to change as conditions on a reef do. The results of Rassweiler *et al.* suggest that the taxa preferred by fishers operating are different on healthy reefs and on degraded, macroalgae-dominated reefs, and imply that shifts towards macroalgae dominance could be accompanied by greater harvesting of rabbitfish [62]. Fishers in the Solomon Islands have also successfully responded in the past to the evolution of conditions in local fishing areas, by a combination of altering which gear and methods they used, which species they targeted, and which locations they visited [63]. Hence, implementing flexible harvesting practices in response to greater sedimentation on reefs can be informed by local knowledge of which species to target under turbid conditions.

One potential application of our work is to inform policy on changing fishing practices to minimize risk of fisheries collapse. Our model can identify which fish functional groups will likely be more robust in the future; hence, the harvesting of such species could be subsidized. Future work will therefore include using a coupled human-environment approach [64] to model fish yields on reefs in which environmental conditions and fishing policy are both changing.

Ethics

This work did not require ethical approval from a human subject or animal welfare committee.

Data accessibility

All data used for model parametrization is taken from previous publications. The code for simulating the model is on Zenodo (DOI: 10.5281/zenodo.7036364).

Declaration of AI use

We have not used AI-assisted technologies in creating this article.

Competing interests

The authors declare no competing interests.

Funding

This research was funded by NSERC Discovery Grants awarded to CTB and to MA.

References

[1] K. E. Fabricius, Factors determining the resilience of coral reefs to eutrophication: A review and conceptual model, in: Coral Reefs: An Ecosystem in Transition, Springer Netherlands, 2010, pp. 493–505. doi:10.1007/978-94-007-0114-4_28.

[2] M. J. Risk, Assessing the effects of sediments and nutrients on coral reefs, Current Opinion in Environmental Sustainability 7 (2014) 108–117. doi:10.1016/j.cosust.2014.01.003.

[3] C. H. R. Goatley, R. M. Bonaldo, R. J. Fox, D. R. Bellwood, Sediments and herbivory as sensitive indicators of coral reef degradation, Ecology and Society 21 (1) (2016). doi:10.5751/es-08334-210129.

[4] A. S. Wenger, K. E. Fabricius, G. P. Jones, J. E. Brodie, Effects of sedimentation, eutrophication, and chemical pollution on coral reef fishes, in: C. Mora (Ed.), Ecology of Fishes on Coral Reefs, Cambridge University Press, 2015, pp. 145–153. doi:10.1017/cbo9781316105412.017.

[5] J. Maina, H. de Moel, J. Zinke, J. Madin, T. McClanahan, J. E. Vermaat, Human deforestation outweighs future climate change impacts of sedimentation on coral reefs, Nature Communications 4 (1) (2013). doi:10.1038/ncomms2986.

[6] R. J. Hamilton, G. R. Almany, C. J. Brown, J. Pita, N. A. Peterson, J. H. Choat, Logging degrades nursery habitat for an iconic coral reef fish, Biological Conservation 210 (2017) 273–280. doi:10.1016/j.biocon.2017.04.024.

[7] M. D. Smith, C. A. Roheim, L. B. Crowder, B. S. Halpern, M. Turnipseed, J. L. Anderson, F. Asche, L. Bourillón, A. G. Guttormsen, A. Khan, L. A. Liguori, A. McNevin, M. I. O'Connor, D. Squires, P. Tyedmers, C. Brownstein, K. Carden, D. H. Klinger, R. Sagarin, K. A. Selkoe, Sustainability and global seafood, Science 327 (5967) (2010) 784–786. doi:10.1126/science.1185345.

[8] R. Bartley, Z. T. Bainbridge, S. E. Lewis, F. J. Kroon, S. N. Wilkinson, J. E. Brodie, D. M. Silburn, Relating sediment impacts on coral reefs to watershed sources, processes and management: A review, Science of The Total Environment 468-469 (2014) 1138–1153. doi:10.1016/j.scitotenv.2013.09.030.

[9] D. T. Neil, A. R. Orpin, P. V. Ridd, B. Yu, Sediment yield and impacts from river catchments to the Great Barrier Reef lagoon: a review, Marine and Freshwater Research 53 (4) (2002) 733. doi:10.1071/mf00151.

[10] A. S. Wenger, S. Atkinson, T. Santini, K. Falinski, N. Hutley, S. Albert, N. Horning, J. E. M. Watson, P. J. Mumby, S. D. Jupiter, Predicting the impact of logging activities on soil erosion and water quality in steep, forested tropical islands, Environmental Research Letters 13 (4) (2018) 044035. doi:10.1088/1748-9326/aab9eb.

[11] S. B. Tebbett, D. R. Bellwood, Algal turf sediments on coral reefs: what's known and what's next, Marine Pollution Bulletin 149 (2019) 110542. doi:10.1016/j.marpolbul.2019.110542.

[12] G. R. Russ, S.-L. A. Questel, J. R. Rizzari, A. C. Alcala, The parrotfish–coral relationship: refuting the ubiquity of a prevailing paradigm, Marine Biology 162 (10) (2015) 2029–2045. doi:10.1007/s00227-015-2728-3.

[13] J. M. S. Delevaux, S. D. Jupiter, K. A. Stamoulis, L. L. Bremer, A. S. Wenger, R. Dacks, P. Garrod, K. A. Falinski, T. Ticktin, Scenario planning with linked land-sea models inform where forest conservation actions will promote coral reef resilience, Scientific Reports 8 (1) (2018). doi:10.1038/s41598-018-29951-0.

[14] A. S. Wenger, D. Harris, S. Weber, F. Vaghi, Y. Nand, W. Naisilisili, A. Hughes, J. Delevaux, C. J. Klein, J. Watson, P. J. Mumby, S. D. Jupiter, Best-practice forestry management delivers diminishing returns for coral reefs with increased land-clearing, Journal of Applied Ecology 57 (12) (2020) 2381–2392. doi:10.1111/1365-2664.13743.

[15] C. Boström, S. Pittman, C. Simenstad, R. Kneib, Seascape ecology of coastal biogenic habitats: advances, gaps, and challenges, Marine Ecology Progress Series 427 (2011) 191–217. doi:10.3354/meps09051.

[16] M. I. Saunders, S. Atkinson, C. J. Klein, T. Weber, H. P. Possingham, Increased sediment loads cause non-linear decreases in seagrass suitable habitat extent, PLOS ONE 12 (11) (2017) e0187284. doi:10.1371/journal.pone.0187284.

[17] D. L. A. Gaveau, D. Sheil, Husnayaen, M. A. Salim, S. Arjasakusuma, M. Ancrenaz, P. Pacheco, E. Meijaard, Rapid conversions and avoided deforestation: examining four decades of industrial plantation expansion in Borneo, Scientific Reports 6 (1) (2016). doi:10.1038/srep32017.

[18] J. R. King, G. A. McFarlane, Marine fish life history strategies: applications to fishery management, Fisheries Management and Ecology 10 (4) (2003) 249–264. doi:10.1046/j.1365-2400.2003.00359.x.

[19] R. Marriott, B. Mapstone, G. Begg, Age-specific demographic parameters, and their implications for management of the red bass, Lutjanus bohar (Forsskal 1775): A large, long-lived reef fish, Fisheries Research 83 (2-3) (2007) 204–215. doi:10.1016/j.fishres.2006.09.016.

[20] M. McLean, D. Mouillot, A. Auber, Ecological and life history traits explain a climate-induced shift in a temperate marine fish community, Marine Ecology Progress Series 606 (2018) 175–186. doi:10.3354/meps12766.

[21] G. Gellner, K. McCann, A. Hastings, Stable diverse food webs become more common when interactions are more biologically constrained, Proceedings of the National Academy of Sciences 120 (31) (2023) e2212061120.

[22] C. Vancutsem, F. Achard, J.-F. Pekel, G. Vieilledent, S. Carboni, D. Simonetti, J. Gallego, L. E. O. C. Aragão, R. Nasi, Long-term (1990–2019) monitoring of forest cover changes in the humid tropics, Science Advances 7 (10) (2021). doi:10.1126/sciadv.abe1603.

[23] J. Gibson, Forest loss and economic inequality in the Solomon Islands: Using small-area estimation to link environmental change to welfare outcomes, Ecological Economics 148 (2018) 66–76. doi:10.1016/j.ecolecon.2018.02.012.

[24] S. Albert, N. Deering, S. Tongi, A. Nandy, A. Kisi, M. Sirikolo, M. Maehaka, N. Hutley, S. Kies-Ryan, A. Grinham, Water quality challenges associated with industrial logging of a karst landscape: Guadalcanal, Solomon Islands, Marine Pollution Bulletin 169 (2021) 112506. doi:10.1016/j.marpolbul.2021.112506.

[25] E. Katovai, A. L. Burley, M. M. Mayfield, Understory plant species and functional diversity in the degraded wet tropical forests of Kolombangara Island, Solomon Islands, Biological Conservation 145 (1) (2012) 214–224. doi:10.1016/j.biocon.2011.11.008.

[26] S. Huo, M. Wang, G. Chen, H. Shu, R. Yang, Monitoring and assessment of endangered UNESCO world heritage sites using space technology: a case study of East Rennell, Solomon Islands, Heritage Science 9 (1) (2021). doi:10.1186/s40494-021-00574-5.

[27] T. Furusawa, K. Pahari, M. Umezaki, R. Ohtsuka, Impacts of selective logging on New Georgia Island, Solomon Islands evaluated using very-high-resolution satellite (IKONOS) data, Environmental Conservation 31 (4) (2004) 349–355. doi:10.1017/s0376892904001638.

[28] B. S. Halpern, K. A. Selkoe, C. White, S. Albert, S. Aswani, M. Lauer, Marine protected areas and resilience to sedimentation in the Solomon Islands, Coral Reefs 32 (1) (2012) 61–69. doi:10.1007/s00338-012-0981-1.

[29] S. M. Ross, A. Dykes, Soil conditions, erosion and nutrient loss on steep slopes under mixed dipterocarp forest in Brunei Darussalam, in: Monographiae Biologicae, Springer Netherlands, 1996, pp. 259–270. doi:10.1007/978-94-009-1685-2_24.

[30] R. C. Sidle, A. D. Ziegler, J. N. Negishi, A. R. Nik, R. Siew, F. Turkelboom, Erosion processes in steep terrain—truths, myths, and uncertainties related to forest management in Southeast Asia, Forest Ecology and Management 224 (1-2) (2006) 199–225. doi:10.1016/j.foreco.2005.12.019.

[31] H. Hartanto, R. Prabhu, A. S. Widayat, C. Asdak, Factors affecting runoff and soil erosion: plot-level soil loss monitoring for assessing sustainability of forest management, Forest Ecology and Management 180 (1-3) (2003) 361–374. doi:10.1016/s0378-1127(02)00656-4.

[32] A. D. Ziegler, T. W. Giambelluca, L. T. Tran, T. T. Vana, M. A. Nullet, J. Fox, T. D. Vien, J. Pinthong, J. Maxwell, S. Evett, Hydrological consequences of landscape fragmentation in mountainous northern Vietnam: evidence of accelerated overland flow generation, Journal of Hydrology 287 (1-4) (2004) 124–146. doi:10.1016/j.jhydrol.2003.09.027.

[33] N. Hutley, M. Boselalu, A. Wenger, A. Grinham, B. Gibbes, S. Albert, Evaluating the effect of data-richness and model complexity in the prediction of coastal sediment loading in Solomon Islands, Environmental Research Letters 15 (12) (2020) 124044. doi:10.1088/1748-9326/abc8ba.

[34] T. D. Brewer, J. E. Cinner, R. Fisher, A. Green, S. K. Wilson, Market access, population density, and socioeconomic development explain diversity and functional group biomass of coral reef fish assemblages, Global Environmental Change 22 (2) (2012) 399–406. doi:10.1016/j.gloenvcha.2012.01.006.

[35] Y. Stender, P. L. Jokiel, K. S. Rodgers, Thirty years of coral reef change in relation to coastal construction and increased sedimentation at Pelekane Bay, Hawai'i, PeerJ 2 (2014) e300. doi:10.7717/peerj.300.

[36] T. Shinnaka, M. Sano, K. Ikejima, P. Tongnunui, M. Horinouchi, H. Kurokura, Effects of mangrove deforestation on fish assemblage at Pak Phanang Bay, southern Thailand, Fisheries Science 73 (4) (2007) 862–870. doi:10.1111/j.1444-2906.2007.01407.x.

[37] J. O. Zeni, M. A. Pérez-Mayorga, C. A. Roa-Fuentes, G. L. Brejão, L. Casatti, How deforestation drives stream habitat changes and the functional structure of fish assemblages in different tropical regions, Aquatic Conservation: Marine and Freshwater Ecosystems 29 (8) (2019) 1238–1252. doi:10.1002/aqc.3128.

[38] A. Kamdem Toham, G. G. Teugels, First data on an index of biotic integrity (IBI) based on fish assemblages for the assessment of the impact of deforestation in a tropical West African river system, Hydrobiologia 397 (1998) 29–38. doi:10.1023/a:1003605801875.

[39] E. B. D. Jones, G. S. Helfman, J. O. Harper, P. V. Bolstad, Effects of riparian forest removal on fish assemblages in southern Appalachian streams, Conservation Biology 13 (6) (1999) 1454–1465. doi:10.1046/j.1523-1739.1999.98172.x.

[40] United Nations, Department of Economic and Social Affairs, Population Division, World population prospects 2019: Online edition (2019).
URL https://population.un.org/wpp/Download/

[41] J. C. Selgrath, S. E. Gergel, A. C. J. Vincent, Incorporating spatial dynamics greatly increases estimates of long-term fishing effort: a participatory mapping approach, ICES Journal of Marine Science 75 (1) (2017) 210–220. doi:10.1093/icesjms/fsx108.

[42] K. R. Stewart, R. L. Lewison, D. C. Dunn, R. H. Bjorkland, S. Kelez, P. N. Halpin, L. B. Crowder, Characterizing fishing effort and spatial extent of coastal fisheries, PLoS ONE 5 (12) (2010) e14451. doi:10.1371/journal.pone.0014451.

[43] S. Tanaka, R. Nishii, A model of deforestation by human population interactions, Environmental and Ecological Statistics 4 (1) (1997) 83–92. doi:10.1023/a:1018510125512.

[44] G. Vieilledent, C. Grinand, R. Vaudry, Forecasting deforestation and carbon emissions in tropical developing countries facing demographic expansion: a case study in Madagascar, Ecology and Evolution 3 (6) (2013) 1702–1716. doi:10.1002/ece3.550.

[45] Q. V. Khuc, B. Q. Tran, P. Meyfroidt, M. W. Paschke, Drivers of deforestation and forest degradation in Vietnam: An exploratory analysis at the national level, Forest Policy and Economics 90 (2018) 128–141. doi:10.1016/j.forpol.2018.02.004.

[46] C. R. Fong, S. J. Bittick, P. Fong, Simultaneous synergist, antagonistic and additive interactions between multiple local stressors all degrade algal turf communities on coral reefs, Journal of Ecology 106 (4) (2018) 1390–1400. doi:10.1111/1365-2745.12914.

[47] J. I. Ellis, T. Jamil, H. Anlauf, D. J. Coker, J. Curdia, J. Hewitt, B. H. Jones, G. Krokos, B. Kürten, D. Hariprasad, F. Roth, S. Carvalho, I. Hoteit, Multiple stressor effects on coral reef ecosystems, Global Change Biology 25 (12) (2019) 4131–4146. doi:10.1111/gcb.14819.

[48] T. Fung, R. M. Seymour, C. R. Johnson, Alternative stable states and phase shifts in coral reefs under anthropogenic stress, Ecology 92 (4) (2011) 967–982. doi:10.1890/10-0378.1.

[49] C. H. R. Goatley, D. R. Bellwood, Sediment suppresses herbivory across a coral reef depth gradient, Biology Letters 8 (6) (2012) 1016–1018. doi:10.1098/rsbl.2012.0770.

[50] S. B. Tebbett, C. H. Goatley, R. P. Streit, D. R. Bellwood, Algal turf sediments limit the spatial extent of function delivery on coral reefs, Science of The Total Environment 734 (2020) 139422. doi:10.1016/j.scitotenv.2020.139422.

[51] Y. Tao, J. Ren, The stability and bifurcation of homogeneous diffusive predator–prey systems with spatio–temporal delays, Discrete & Continuous Dynamical Systems-B 27 (1) (2022) 229.

[52] A. S. Hoey, D. R. Bellwood, Cross-shelf variation in the role of parrotfishes on the Great Barrier Reef, Coral Reefs 27 (1) (2007) 37–47. doi:10.1007/s00338-007-0287-x.

[53] F. X. Latrille, S. B. Tebbett, D. R. Bellwood, Quantifying sediment dynamics on an inshore coral reef: Putting algal turfs in perspective, Marine Pollution Bulletin 141 (2019) 404–415. doi:10.1016/j.marpolbul.2019.02.071.

[54] A. L. Downing, B. L. Brown, E. M. Perrin, T. H. Keitt, M. A. Leibold, Environmental fluctuations induce scale-dependent compensation and increase stability in plankton ecosystems, Ecology 89 (11) (2008) 3204–3214. doi:10.1890/07-1652.1.

[55] Y. Tao, S. A. Campbell, F. J. Poulin, Dynamics of a diffusive nutrient-phytoplankton-zooplankton model with spatio-temporal delay, SIAM Journal on Applied Mathematics 81 (6) (2021) 2405–2432.

[56] R. Froese, D. Pauly, Fishbase, www.fishbase.org (2022).

[57] M. Moustaka, T. J. Langlois, D. McLean, T. Bond, R. Fisher, P. Fearns, P. Dorji, R. D. Evans, The effects of suspended sediment on coral reef fish assemblages and feeding guilds of north-west Australia, Coral Reefs 37 (3) (2018) 659–673. doi:10.1007/s00338-018-1690-1.

[58] C. C. Hicks, T. R. McClanahan, Assessing gear modifications needed to optimize yields in a heavily exploited, multi-species, seagrass and coral reef fishery, PLoS ONE 7 (5) (2012) e36022. doi:10.1371/journal.pone.0036022.

[59] R. Hilborn, A. E. Punt, J. Orensanz, Beyond band-aids in fisheries management: fixing world fisheries, Bulletin of Marine Science 74 (3) (2004) 493–507.
URL https://www.ingentaconnect.com/content/umrsmas/bullmar/2004/00000074/00000003/art00003

[60] T. McClanahan, Human and coral reef use interactions: From impacts to solutions?, Journal of Experimental Marine Biology and Ecology 408 (1-2) (2011) 3–10. doi:10.1016/j.jembe.2011.07.021.

[61] C. N. T. Quynh, S. Schilizzi, A. Hailu, S. Iftekhar, Fishers' preference heterogeneity and trade-offs between design options for more effective monitoring of fisheries, Ecological Economics 151 (2018) 22–33. doi:10.1016/j.ecolecon.2018.04.032.

[62] A. Rassweiler, S. D. Miller, S. J. Holbrook, M. Lauer, M. A. Strother, S. E. Lester, T. C. Adam, J. Wencélius, R. J. Schmitt, How do fisher responses to macroalgal overgrowth influence the resilience of coral reefs?, Limnology and Oceanography 67 (S1) (2021). doi:10.1002/lno.11921.

[63] S. Albert, S. Aswani, P. L. Fisher, J. Albert, Keeping food on the table: Human responses and changing coastal fisheries in Solomon Islands, PLOS ONE 10 (7) (2015) e0130800. doi:10.1371/journal.pone.0130800.

[64] M. Yodzis, C. T. Bauch, M. Anand, Coupling fishery dynamics, human health and social learning in a model of fish-borne pollution exposure, Sustainability Science 11 (2016) 179–192.

Supporting Information:
Reef fish functional groups show variable declines due to deforestation-driven sedimentation, while flexible harvesting mitigates this damage

Russell Milne[1,2,*,†], Madhur Anand[1,2], Chris T. Bauch[1,2]

1 Department of Applied Mathematics, University of Waterloo, Waterloo, Ontario, Canada
2 School of Environmental Sciences, University of Guelph, Guelph, Ontario, Canada

* Corresponding author. Email address: rmilne@ualberta.ca
† Current address: Department of Mathematical and Statistical Sciences, University of Alberta, Edmonton, Alberta, Canada

A Model construction

A.1 Fish trophic interactions

Since turf algae and macroalgae were assumed to be grazed at rates $g_{_T}$ and $g_{_M} \leq g_{_T}$, respectively, it can be further assumed that the relative proportions of turf algae and macroalgae consumed by grazers (such as herbivorous fish) can be represented with the ratio $\frac{g_{_M}}{g_{_T}} \leq 1$. Hence, we took $T + \frac{g_{_M}}{g_{_T}} M \leq 1$ as the scaling term for herbivorous fish growth. As rates of herbivory are negatively impacted by accumulation of algal turf sediment [1, 2], we introduced another quantity $\mu(t)$ representing this decrease. $\mu(t)$ depends on sediment quantities on the seabed, and is further explained below. We assumed that herbivorous fish would be eaten by piscivorous fish and top predators, with $\delta_{_P}$ denoting the percentage of the diet of piscivores made up by herbivores and $\delta_{_Z}^{H}$ denoting this percentage for top predators. This meant that our scaling constant for herbivorous fish predation was taken to be $\frac{\delta_{_P} F_{_P} + \delta_{_Z}^{H} F_{_Z}}{\delta_{_P} + \delta_{_Z}^{H}} \leq 1$. Therefore, after also accounting for the harvesting term $-h_{_H} F_{_H}$, we represented the differential equation for herbivorous fish as follows:

$$\frac{\mathrm{d}F_{_H}}{\mathrm{d}t} = \frac{r_{_H}}{1+\mu} F_{_H} \left(1 - F_{_H}\right) \left(T + \frac{g_{_M}}{g_{_T}} M\right) - h_{_H} F_{_H} - m_{_H} F_{_H} \frac{\delta_{_P} F_{_P} + \delta_{_Z}^{H} F_{_Z}}{\delta_{_P} + \delta_{_Z}^{H}} \tag{A.1}$$

The diet of omnivorous fish typically consists partly of primary producers (e.g. algae) and partly of other food sources such as zooplankton and small invertebrates [3]. We defined $\delta_{_O}$ as the percentage of an omnivorous fish's diet consisting of algae, and assumed that omnivorous fish would consume turf algae and macroalgae at the same relative rates as herbivorous fish. This was scaled down by μ in the same way as in the dynamics for herbivorous fish. This implies that $(1 - \delta_{_O})$ percent of an onmivorous fish's diet consists of other food sources, the availability of which we modelled using a function $\phi(t)$ (see below). As with herbivorous fish, we assumed that omnivorous fish were eaten by piscivorous fish (composing $(1 - \delta_{_P})$ percent of their diet) and top predators (composing $\delta_{_Z}^{O}$ percent of their diet), and harvested at a constant rate. Therefore, the dynamics of omnivorous fish are represented as follows:

$$\frac{\mathrm{d}F_{O}}{\mathrm{d}t} = r_{O}F_{O}\left(1-F_{O}\right)\left(\frac{\delta_{O}}{1+\mu}\left(T+\frac{g_{M}}{g_{T}}M\right)+\left(1-\delta_{O}\right)\phi\right) - h_{O}F_{O} - m_{O}F_{O}\frac{(1-\delta_{P})F_{P}+\delta_{Z}^{O}F_{Z}}{1-\delta_{P}+\delta_{Z}^{O}} \tag{A.2}$$

As detailed above, piscivorous fish were assumed to eat both herbivorous and omnivorous fish, in proportions δ_{P} and $(1-\delta_{P})$, respectively. They are, in turn, eaten by top predators and harvested. Note that the proportion of top predator diet that piscivorous fish make up is $1-\delta_{Z}^{H}-\delta_{Z}^{O}$. As the total predation pressure on piscivorous fish is therefore $F_{Z}\left(1-\delta_{Z}^{H}-\delta_{Z}^{O}\right)$, but scaling this to values between 0 and 1 involves dividing by $1-\delta_{Z}^{H}-\delta_{Z}^{O}$, this constant is normalized out of the differential equation governing piscivorous fish dynamics. The differential equation in question is as follows:

$$\frac{\mathrm{d}F_{P}}{\mathrm{d}t} = r_{P}F_{P}\left(1-F_{P}\right)\left(\delta_{P}F_{H}+\left(1-\delta_{P}\right)F_{O}\right) - h_{P}F_{P} - m_{P}F_{P}F_{Z} \tag{A.3}$$

Top predators consume fish from all other functional groups, according to the proportions mentioned above. As they lack predators by definition, the sources of their mortality are assumed to be harvesting and natural causes. This yields the following differential equation for top predators:

$$\frac{\mathrm{d}F_{Z}}{\mathrm{d}t} = r_{Z}F_{Z}\left(1-F_{Z}\right)\left(\delta_{Z}^{H}F_{H}+\delta_{Z}^{O}F_{O}+\left(1-\delta_{Z}^{H}-\delta_{Z}^{O}\right)F_{P}\right) - h_{Z}F_{Z} \tag{A.4}$$

Fung *et al.* did not explicitly include grazer populations in their model, and hence represented grazing pressure as a constant θ. We instead use a baseline rate $\tilde{\theta}$ scaled by the population levels of herbivorous and omnivorous fish relative to their theoretical maxima, with the contribution of omnivorous fish to grazing being the proportion of their diet consisting of algae. The grazing rate also decreases as sediment levels increase, so we additionally divide by $1+\mu$ (as in the grazing terms of F_{H} and F_{O}) to represent this. Specifically, we take θ to be the following:

$$\theta(t) = \frac{\tilde{\theta}\left(F_{H}+\delta_{O}F_{O}\right)}{\left(1+\mu\right)\left(1+\delta_{O}\right)} \tag{A.5}$$

A.2 Deforestation and sediment dynamics

Changes in forest cover were modelled in a variety of different ways, to represent unmanaged deforestation and managed logging. For our baseline scenario, we assumed a steady loss of forest cover scaling with population increases. Here, we drew on the work of Tanaka and Nishii [4] which modelled the percentage change in forest cover per unit change in area population; we defined r_{X} as the linear rate of deforestation referred to as r in [4]. We used United Nations population growth estimates for the Solomon Islands [5] to obtain values for population N and population change $\frac{\mathrm{d}N}{\mathrm{d}t}$. We also assumed a background rate of forest regrowth, governed by the rate a_{X}. We took the forest regrowth term to be logistic, as the rate of forest expansion into cleared land should decrease as the amount of available cleared land does; we assumed a carrying capacity of 1, or 100% forest cover. Therefore, the differential equation for forest cover, $\frac{\mathrm{d}X}{\mathrm{d}t}$, was taken to be the following:

$$\frac{\mathrm{d}X}{\mathrm{d}t} = \frac{\mathrm{d}X}{\mathrm{d}N}\frac{\mathrm{d}N}{\mathrm{d}t} + a_{X}X(1-X) = -r_{X}NX\frac{\mathrm{d}N}{\mathrm{d}t} + a_{X}X(1-X) \tag{A.6}$$

Sediment export onto reefs was assumed to change due to deforestation, and specifically increase due to increased erosion when forest cover was low. The amount of sediment being deposited onto

reefs due to soil erosion typically increases linearly as forest cover is reduced [6, 7]. We took q_b to be the baseline river sediment concentration at 100 percent forest cover, and q_c to represent the additional amount of sediment in rivers when all land has been cleared; both of these have units of mg cm^{-3}. We also took λ (measured in yr^{-1}) as the rate at which sediment in these rivers is exported into the water column. Once sediment is suspended in the water column above a reef, it can be washed out further into the ocean or settle on the seabed. We took e to be the rate at which sediment is washed out of a reef ecosystem, and assumed that the amount of sediment on the seabed would be in equilibrium with the amount suspended in the water column. The differential equation for S_W is therefore as follows:

$$\frac{\mathrm{d}S_W}{\mathrm{d}t} = \left(q_b + (1 - X)\, q_c\right) \lambda - eS_W \tag{A.7}$$

Here, the term eS_W covers both initial export of sediment by rivers to areas beyond a reef (which first must physically pass through the reef area) and later off-shelf export of sediment in the water above a reef. This was done since both of these processes are significant [8, 9] and data that could be used to separate the two was not readily available. Because suspended sediment and sediment on the seabed are measured in different units (mass per unit volume and per unit area, respectively), and converting between these may be difficult, we opted to express sediment on the seabed as a ratio between the level at any given time and levels corresponding to pristine conditions. A corollary of our assumption that accumulated seabed sediment is in equilibrium with suspended sediment concentration is that the growth in these two variables is proportional to each other, and expressing S_B as a ratio (i.e. indexing a value of $S_B = 1$ to pristine conditions) rather than as a differential equation eliminates the need for a growth rate constant. We therefore took S_B to be the following:

$$S_B\left(t\right) = \frac{S_W\left(t\right)}{S_W\left(t = 0\right)} \tag{A.8}$$

Fung *et al.* identified sedimentation as affecting four processes in their model, namely lateral coral growth (described using r_C), larval recruitment of both local brooding and exogenous spawning corals (l_C^b and l_C^s, respectively), and coral death (d_C). The existing literature describes changes in these processes as functions of sedimentation rates, rather than the total amount of sediment either in the water column or on the seabed (see e.g. [10] Appendix B). We therefore assumed that these processes could be described as baseline rates $\tilde{r}_C$, $\tilde{l}_C^b$, $\tilde{l}_C^s$, and $\tilde{d}_C$ scaled up or down according to the sedimentation rate. Much of the redistribution of sediment on reefs is performed by parrotfish [11, 12], which bite into sediment while feeding and therefore reduce sediment buildup on reefs, lowering the effective sedimentation rate, although other herbivorous fish with different feeding methods also may have effects on sediment accumulation [12]. In a recent experiment in which areas of seabed were caged off to simulate a herbivorous fish density of zero, Akita *et al.* found that the caged areas had on average double the accumulated sediment levels compared to uncaged control sites [13]. All of the control sites in [13] were fished, and herbivorous fish landings in the area were reported as being half of what was caught in the 1990s, suggesting that herbivorous fish density there would be at most half of its theoretical maximum. Since the sedimentation rates (mass per unit area per unit time) observed by [13] were similar to pristine values observed elsewhere (see below), we therefore assumed that the sedimentation rate would begin linearly increasing when the herbivorous fish population declined below a value of 0.5, and would double when no herbivorous fish were present. Hence, we defined the sedimentation rate as follows:

$$r_{\text{Sed}} = \max[1 + (1 - 2H), 1]\, k_{\text{Dep}} S_W \tag{A.9}$$

This formulation uses a constant k_{Dep} to represent the baseline rate of sediment deposition, as well as incorporating dependence on the population of herbivorous fish. (We took k_{Dep} to have units of $100 \times$ cm yr^{-1}. This is done so that the rate of sedimentation is expressed over an area rather than a volume, and hence can be calibrated to observed field values that are measured in mg cm^{-2} time^{-1}. The scaling down of k_{Dep} by a factor of 100 was done because the field data on sedimentation rates that we fit our model to had time units of days, while time in our model is expressed in years, and we intended to keep our sedimentation rate on the same order of magnitude as the raw numbers seen in the field.) Because the three coral growth processes were negatively affected by sedimentation, we modelled them as follows:

$$r_C(t) = \frac{\tilde{r}_C \kappa_r}{\kappa_r + r_{\text{Sed}}}; \quad l^b_C(t) = \frac{\tilde{l}^b_C \kappa_b}{\kappa_b + r_{\text{Sed}}}; \quad l^s_C(t) = \frac{\tilde{l}^s_C \kappa_s}{\kappa_s + r_{\text{Sed}}} \tag{A.10}$$

Here, κ_r, κ_b, and κ_s are constants that determine at which sedimentation rate the corresponding coral growth rate is halved. Coral death instead increases when sedimentation rate is high. This means that the sedimentation-dependent coral death rate can be taken as the following, with κ_d a scaling constant:

$$d_C(t) = \tilde{d}_C \left(1 + \frac{r_{\text{Sed}}}{\kappa_d}\right) \tag{A.11}$$

In addition to sedimentation's effects on coral, the buildup of algal turf sediment (i.e. sediment on the seabed contained under and within areas dominated by algal turf) is known to inhibit herbivory of algae [1, 2]. As mentioned above, we modelled this by using a factor μ to divide the rates of grazing and herbivory in the model. We assume here that sediment is evenly distributed on the seabed, so the amount of sediment accumulated there is a good proxy for algal turf sediment, and hence the extent to which local algal turf is closer to being SPAT (short, productive algal turf, the kind preferred by herbivorous fish) or LSAT. This can be done because the correlation between seabed sediment load and algal turf length is roughly linear [2]. Tebbett *et al.* found that approximately doubling seabed sediment concentration from pristine values led to herbivorous fish bites on algae approximately halving, and a quadrupling of sediment concentration led to a 78% reduction in herbivorous fish bites compared to the pristine baseline (i.e. approximately another halving from the value with doubled sediment levels) [2]. Similarly, it has been found that removal of large amounts of sediment from reef flats (where seabed sediment buildup is greater) had similar effects on encouraging herbivory as removing much smaller amounts of sediment from reef areas with less sediment buildup [1], indicating the sensitivity of herbivorous fish to algal turf sediment levels. Because of this, we assumed that μ would increase logarithmically with the amount of sediment on the seabed, with a logarithm base of 2 due to the repeated halvings mentioned above. This means that our formulation for μ is as follows:

$$\mu = \max[\log_2(S_B), 0] \tag{A.12}$$

Much of the diet of omnivorous fish consists of zooplankton [3]. The phytoplankton that zooplankton eat can have their population growth limited by low light availability, such as in turbid waters, making planktonic food webs vulnerable to suspended sediment increases [14]. Zooplankton dynamics (and hence zooplankton-phytoplankton trophic interactions) happen over a faster

timescale than the rest of the processes in our model [15], and plankton population dynamics are also less complex in more active waters [16] such as those near the mouth of a river. Therefore, we assumed a direct dependence of $\phi(t)$ on suspended sediment concentration. This involved scaling ϕ with light availability according to the Lambert-Beer law [17], which is the following function relating underwater light intensity I to intensity of the light source I_0, depth d, and light attenuation constant k_{att}:

$$I = I_0 e^{-k_{\text{att}} d} \tag{A.13}$$

We took the light attenuation constant k_{att} to vary based on suspended sediment concentration. A linear relationship has been found between these two quantities in estuarine waters [18], which has a slope of 60 when suspended sediments are measured in mg cm^{-3}. Furthermore, we assumed that $\phi = 1$ in pristine conditions (to bound the growth rate of omnivorous fish above by 1), and that water depth was constant. These constraints meant that we took the following form for ϕ:

$$\phi = \exp\Big(-\tilde{\phi} S_W\Big); \quad \tilde{\phi} = 60 \tag{A.14}$$

Algae on the seabed also undergoes photosynthesis, and coral obtains much of its energy from dinoflagellate symbionts, which in turn get their energy from photosynthesis. However, the reduction in coral growth and reproduction rates due to sedimentation (including from photosynthesis reduction) is already included in the model via processes detailed by Fung *et al.* (see above). Additionally, Fung *et al.* considered reduction in algal photosynthesis due to sedimentation, but did not include it in their model due to lack of data. We also opted not to include this. Turf algae spread very rapidly, and have been found to dominate the benthos under conditions featuring high turbidity [19] or sedimentation rates [20, 21] due to their ability to trap sediment. Therefore, we assumed that although light attenuation due to turbidity may affect the growth of turf algae, it would not appreciably affect their spread if a reasonable amount of light still reached the seabed. Conversely, the steady-state macroalgae levels reached with our baseline parameter values were low enough that any difference due to decreasing photosynthesis would be minimal.

B Model parametrization

All parameters relating to transitions on the seabed between coral, macroalgae, turf algae and space that were used by Fung *et al.* were kept at the values specified in [10]. This includes the baseline values $\tilde{\theta}$, $\tilde{r}_C$, $\tilde{l}^b_C$, $\tilde{l}^s_C$, and $\tilde{d}_C$ for rates affected by features that we added to the model.

Growth and harvesting rates for each fish functional group, as well as diet composition ratios for omnivorous and piscivorous fish, were taken from FishBase [3]. This involved first dividing all reef-associated fish species observed in our study region (the Solomon Islands) for which data on both doubling time and use by fisheries was available into functional groups depending on their trophic level. Fish with a listed trophic level of 2.0 were assumed to be herbivorous, those with tropic level greater than 2.0 but less than 3.0 were assumed to be omnivorous (with a diet consisting partially of algae and partially of alternative sources such as invertebrates), those with trophic level at least 3.0 but less than 4.0 were assumed piscivorous due to being a full trophic level above herbivorous fish, and those with trophic level at least 4.0 were designated top-level predators. (The fish in the latter two categories could include some predators of benthic crustaceans as well as predators of

fish. Hence, during our calculations below, we assumed that growth and harvesting rates would be similar between those groups.)

The omnivorous fish species for which growth and harvesting data was available had an average trophic level of 2.62, while that of the piscivorous species (other than top predators) was 3.49. Therefore, we took $\delta_{_O} = 0.38$ and $\delta_{_P} = 0.21$ under the assumptions that the diet of omnivorous fish would be 38% algae and 62% organisms that eat algae, and that the diet of piscivorous fish would consist of organisms with an average trophic level of 2.49, such as 21% herbivorous fish (trophic level 2) and 79% omnivorous fish (trophic level 2.62). We took the values of the top predator diet parameters to be $\delta_{_Z}^{H} = 0.1$ and $\delta_{_Z}^{O} = 0.3$. This was based on the assumption that top predators would eat more fish in higher trophic levels, as well as the fact that summing the trophic levels of herbivorous, omnivorous and piscivorous fish with these weights results in a trophic level of 3.08, close to the trophic level of the prey of top predators in the Solomon Islands (3.18).

The intrinsic growth rate for each functional group was set to be the average of those for each species within the functional group, while the growth rate for each species was derived from its reported doubling time using the formula $r = \frac{\ln 2}{t_{_D}}$. As the doubling time of each species was defined using an estimated range, numerical values for each species were obtained by taking the median of this range; if the doubling time for a species was defined as being very long, without an upper bound, this numerical value was taken to be 15 years. These intrinsic growth rates were assumed to hold for pristine reefs, which typically have about 50 percent coral cover [22] that is not edible by herbivorous fish. Therefore, we multiplied each growth rate by 2, so that herbivorous fish growth would scale based on the amount of algae present compared to its observed maximum values on pristine reefs, and the timescale of the other fish functional groups' dynamics (compared to those of herbivorous fish) would not be affected. From this, we obtained $r_{_H} = 1.51$, $r_{_O} = 1.36$, $r_{_P} = 1.45$, and $r_{_Z} = 0.69$.

The harvesting rate for each functional group was defined in the same way, based an average of harvesting rates for each species in the group. A species was assumed to have a harvesting rate of 0.5 if its use by fisheries was listed as "highly commercial", as many highly-fished species have harvesting rates at or above 50 percent annually [23]. Species whose fisheries usage was listed as "commercial" were assumed to have harvesting rates of 0.3, a value that previous modelling studies have determined to be close to the maximum rate at which fish populations can maintain themselves [24, 25], and "minor commercial" species were assumed to have harvesting rates half of that (0.15). The harvesting rate for species that were listed as being the targets of subsistence fishing (rather than commercial fishing) was taken to be 0.05, an order of magnitude lower than the highest commercial rates [26], and species of no commercial interest had a harvesting rate of 0. This process gave us $h_{_H} = 0.2$, $h_{_O} = 0.11$, $h_{_P} = 0.15$, and $h_{_Z} = 0.22$.

Sediment export onto reefs due to erosion is low in heavily forested areas, and increases with the proportion of cleared land [6, 7]. A recent survey on Isabel Island in the Solomon Islands found that over a catchment covered almost entirely by forest, sediment concentrations at the mouth of a local river (the Jejevo) had a geometric mean of 20 mg L^{-1}, or 0.02 mg cm^{-3} [27]. Since the waters at the mouth of the Jejevo have been found to be on average 15 times more turbid than those by adjacent rivers [28], we took $q_{_b}$ to have a high value of 0.02 mg cm^{-3} and a low value of 0.0013 mg cm^{-3}. In the wet tropics of northern Queensland, Australia, Neil *et al.* found a linear relationship between percentage of land cleared and suspended sediment concentration in local rivers during the wet seasons of specific years [6], thus controlling for temporal variation due to any ongoing changes in land use. Plugging 100 percent land clearance into the formulas in [6] yielded values of 72 and 14 mg L^{-1} for very wet and fairly wet conditions, respectively. Wenger *et al.* performed a similar

analysis on Kolombangara Island in the Solomon Islands, based on future predictions of yearly erosion with varying percentages of cleared land [7]. That study found average suspended sediment concentration in streams to be 124 mg L^{-1} at 40 percent cleared land with no management, as well as a linear rate of increase for sediments, implying a concentration of 310 mg L^{-1} when land is fully cleared. The concentration at 100 percent forest cover found by Wenger *et al.* was similar to that found by Neil *et al.*; the difference in slope of the two relationships can be attributed to the fact that Wenger *et al.* considered deforestation on steeper terrain. We therefore took q_c to be 0.31 mg cm^{-3} when simulating deforestation on steep terrain, and 0.043 mg cm^{-3} (the average of the two values found by Neil *et al.*) for gentler terrain. This represents the increase in sedimentation due to erosion that an entirely cleared environment has compared to an entirely forested one.

Rates of sediment export from coastal into off-shelf areas have a great deal of spatial variation (see [8] for an example of this in New Guinea, with both very high and very low amounts of off-shelf export observed). Therefore, we took e to vary over a wide range, namely from 0.1 to 0.9, with the median value 0.5 used as a baseline. We assumed λ to be 1 yr^{-1} in order to simulate conditions on reefs near river mouths. Reefs further away can receive substantially less sediment from river discharges [29]; this process was folded into e in order to simplify the model analysis (see above), as e and λ perform similar functions (limiting sediment on reefs due to local hydrodynamics).

To find a value of k_{Dep} suitable for the Solomon Islands, we related suspended sediment concentrations to rates of sedimentation in a dataset covering Isabel Island [28], using the formula $r_{\text{Sed}} \approx k_{\text{Dep}} S_W$ in the absence of data on parrotfish abundance. We used the average reported turbidity in nephelometric turbidity units (NTUs) at the Jihro inshore reef site in that dataset, which was similar to those on other inshore reefs globally [28] such as on the Great Barrier Reef [12], to estimate suspended sediment concentration. A value in mg L^{-1} was obtained from this using a linear method used in [30], taking the average slope of 18 linear functions linking NTUs to sediment density, and this was further scaled to units of mg cm^{-3}. We then divided the observed sedimentation rates on inshore reefs in this dataset by the obtained average sediment concentration. This gave us an average value of 4400 for k_{Dep}, after disregarding an outlier, which had a sedimentation rate over 20 times higher than the other sites and was therefore deemed non-representative.

While parametrizing their model, Fung *et al.* estimated from field data that a sedimentation rate of 100 mg cm^{-2} d^{-1}, or 365×10^2 mg cm^{-2} yr^{-1}, causes coral lateral growth rate to decline by half (see [10] Appendix B). Hence, we took $\kappa_r = 365$. Similar estimates by Fung *et al.* included that a sedimentation rate of 12 cm^{-2} d^{-1} causes larval recruitment of both brooding and spawning corals to decrease by 60%, and one of 13 cm^{-2} d^{-1} causes coral death rate to double. After converting units, this leads to a value of $\frac{44}{1.5}$ for κ_b and κ_s, and a value of 47.5 for κ_d.

We determined values for r_X by isolating it within the differential equation proposed by Tanaka *et al.* [4], i.e. $\frac{\mathrm{d}F}{\mathrm{d}N} = -r_X F N$. To do this, we used data on deforestation in the Indonesian part of the island of Borneo (i.e. Kalimantan) from 1973 to 2000 and from 2000 to 2010 [31], and population growth data in Kalimantan over the same years [32]. For each of these time periods, we took F to be the percentage forest cover in Kalimantan at the end of the period and N to be the population of Kalimantan at the end of the period relative to its population at the beginning of the period, and estimated $\frac{\mathrm{d}F}{\mathrm{d}N}$ by dividing the change in forest cover by the relative change in population during the period. (2000 and 2010 were census years in Indonesia, and we estimated the 1973 population by assuming a linear rate of growth between the 1971 and 1980 censuses.) We used relative rates rather than absolute population numbers (as was done by Tanaka *et al.*) in order to control for population density and hence maximize applicability to different locations. From these calculations, we obtained a value of 0.18 for r_X from 1973 to 2000, and a value of 0.23 from 2000

to 2010. We therefore took 0.23 as a baseline for r_X, although we allowed it to vary in order to simulate a variety of deforestation speeds.

A long-term study (from 1990 to 2020) on changes in forest cover in the tropics found that out of the undisturbed forest in insular Southeast Asia in 1990, 16.4 percent had been deforested, and 3.7 percent had been deforested and subsequently regrew [33]. This gives an estimate that the speed of reforestation was 0.18 times the speed of deforestation in this time period. Hence, we assumed our background rate of forest regrowth a_X to be 0.18 times the baseline value for r_X of 0.23, or in other words $a_X \approx 0.04$.

C Derivations of harvesting rates

To evaluate the impact of flexible harvesting, we derived a harvesting rate that would change for each functional group based on local availability of fish in that functional group, while the percentage of the total fish population being harvested would remain constant. We first estimated the rate for all functional groups combined by taking a weighted average of the rates h_H, h_O, h_P and h_Z, where the weights were set equal to the relative abundances of each functional group in the initial conditions we specified above. In other words, we defined the aggregate harvesting rate as follows:

$$h_{\text{Tot}} = \frac{h_H F_H(0) + h_O F_O(0) + h_P F_P(0) + h_Z F_Z(0)}{F_H(0) + F_O(0) + F_P(0) + F_Z(0)} \tag{C.15}$$

We then defined a harvesting rate for each functional group based solely on the relative availability of fish in that functional group as follows:

$$h_{\text{Var},I}(t) = \frac{F_I h_{\text{Tot}}}{F_H + F_O + F_P + F_Z}, \quad I \in \{H, O, P, Z\} \tag{C.16}$$

Since some fish species with high abundance (e.g. wrasses) are not expected to be of any commercial interest [34], we did not assume that the actual harvesting rates for each functional group would be solely based on relative fish abundances. Instead, we formulated harvesting rates $\bar{h}_H$, $\bar{h}_O$, $\bar{h}_P$, and $\bar{h}_Z$ for each functional group that would partly depend on the fishing rates parametrized from FishBase (i.e. the intrinsic demand for each functional group) and partially due to local fish availability. In other words, for a constant k_h representing the how important current local conditions are in determining demand for each functional group, we defined each $\bar{h}$ as follows:

$$\bar{h}_I(t) = \frac{h_I + k_h h_{\text{Var},I}}{1 + k_h}, \quad I \in \{H, O, P, Z\} \tag{C.17}$$

We also derived harvesting rates corresponding to constant fishing quotas for each fish functional group. To do this, we assumed that over a unit of time, the total number of fish harvested during that time would always be equal to a value $\rho \times \xi$, where ξ is the number harvested at time $t = 0$ and ρ is a scaling constant. ξ is defined below:

$$\xi = h_H F_H(0) + h_O F_O(0) + h_P F_P(0) + h_Z F_Z(0) \tag{C.18}$$

We further assumed that the different fish functional groups were harvested according to their proportions of the population. This means that, for ω a factor to ensure that the total fish harvested remains constant, the number of fish harvested in each functional group I is as follows:

Param	Value	Units	Description
$r_{_H}$	1.51	yr^{-1}	Intrinsic growth rate for herbivorous fish
$r_{_O}$	1.36	yr^{-1}	Intrinsic growth rate for omnivorous fish
$r_{_P}$	1.45	yr^{-1}	Intrinsic growth rate for piscivorous fish
$r_{_Z}$	0.69	yr^{-1}	Intrinsic growth rate for top predator fish
$h_{_H}$	0.2	yr^{-1}	Harvesting rate for herbivorous fish
$h_{_O}$	0.11	yr^{-1}	Harvesting rate for omnivorous fish
$h_{_P}$	0.15	yr^{-1}	Harvesting rate for piscivorous fish
$h_{_Z}$	0.22	yr^{-1}	Harvesting rate for top predator fish
$m_{_H}$	0.1	yr^{-1}	Mortality due to predation for herbivorous fish
$m_{_O}$	0.1	yr^{-1}	Mortality due to predation for omnivorous fish
$m_{_P}$	0.1	yr^{-1}	Mortality due to predation for piscivorous fish
$\delta_{_O}$	0.38	Unitless	Percentage of omnivorous fish diet consisting of algae
$\delta_{_P}$	0.21	Unitless	Percentage of piscivorous fish diet consisting of herbivorous fish
$\delta_{_Z}^{H}$	0.1	Unitless	Percentage of top predator fish diet consisting of herbivorous fish
$\delta_{_Z}^{O}$	0.3	Unitless	Percentage of top predator fish diet consisting of omnivorous fish
$k_{_h}$	0 - 1	Unitless	Relative importance of local fish availability on harvesting rates
ν	0 - 1	Unitless	Dependence of harvesting on population growth

Table B.1: Parameters related to fish vital processes used in this paper. Mortality rates are assumed based on [24], $k_{_h}$ and ν are allowed to vary over broad potential ranges, and all other parameters are calculated based on FishBase data [3].

Param	Value	Units	Description	Reference
$q_{_b}$	0.0013 - 0.2	mg cm^{-3}	Baseline sediment concentration in rivers due to erosion	[27]
$q_{_c}$	0.043, 0.31	mg cm^{-3}	Additional river sediment concentration when land is 100% cleared	[6, 7]
λ	1	yr^{-1}	Rate at which sediment in rivers is exported to reefs	Assumed
e	0.1 - 0.5 - 0.9	yr^{-1}	Rate at which suspended sediment on reefs leaves the system	[8]
$k_{_{\text{Dep}}}$	4400	$100 \times$ cm yr^{-1}	Constant governing sediment deposition from water column to seabed	[30, 28]
$\kappa_{_r}$	365	$100 \times$ mg cm^{-2} yr^{-1}	Sedimentation rate at which coral lateral growth is halved	[10]
$\kappa_{_b}$	29.2	$100 \times$ mg cm^{-2} yr^{-1}	Sedimentation rate at which brooding coral recruitment is halved	[10]
$\kappa_{_s}$	29.2	$100 \times$ mg cm^{-2} yr^{-1}	Sedimentation rate at which spawning coral recruitment is halved	[10]
$\kappa_{_d}$	47.5	$100 \times$ mg cm^{-2} yr^{-1}	Sedimentation rate at which coral death is doubled	[10]
$\tilde{\phi}$	60	mg^{-1} cm^3	Constant relating non-algal food availability for omnivorous fish and sediment concentration	[18]
$r_{_X}$	0 - 0.23 - 0.25	yr^{-1}	Deforestation rate	[31, 32]
$a_{_X}$	0.18×0.23	yr^{-1}	Forest regrowth rate	[33]

Table B.2: Parameters related to sedimentation used in this paper

$$\left(\frac{F_I}{F_H + F_O + F_P + F_Z}\right)\omega F_I \tag{C.19}$$

In order to obtain ω, we first noted that the number of fish harvested at each time step always being equal to $\rho \times \xi$ implies the following:

$$\sum_I \left(\frac{F_I}{F_H + F_O + F_P + F_Z}\right)\omega F_I = \rho\xi \tag{C.20}$$

By factoring out and isolating ω, we get the following:

$$\omega = \rho\xi\left(\frac{F_H + F_O + F_P + F_Z}{{F_H}^2 + {F_O}^2 + {F_P}^2 + {F_Z}^2}\right) \tag{C.21}$$

The harvesting rate for each functional group I is the number of fish harvested in that functional group divided by its total population. If we denote the harvesting rate as $h^a_{\mathrm{Var},I}$, with the a denoting that the amount harvested is what remains constant, we get the following:

$$h^a_{\mathrm{Var},I} = \frac{\omega F_I}{F_H + F_O + F_P + F_Z} = \frac{\rho\xi F_I}{{F_H}^2 + {F_O}^2 + {F_P}^2 + {F_Z}^2} \tag{C.22}$$

We noted that the denominator of this expression would get very close to zero if all fish species were nearing local extirpation, which was a likely scenario if fishing quotas remained constant. To avoid numerical errors in such a case, we used a modified version of Equation C.17, substituting $h^a_{\mathrm{Var},I}$ in place of $h_{\mathrm{Var},I}$ and taking $k_h = 999$. This gave us variable harvesting rates for each functional group that summed to a generally constant value:

$$\bar{h}_I(t) = \tfrac{1}{1000}\left(h_I + 999h^a_{\mathrm{Var},I}\right), \quad I \in \{H, O, P, Z\} \tag{C.23}$$

As we anticipated that constant harvesting amounts could cause the fish to go extinct, we additionally imposed the constraint while running the model that if the population of a functional group was below 10^{-6}, it would be treated as 0. This constraint further implied that the amount of fish harvested in such cases would also be zero. Calculation of fish extinction time was specifically done for herbivorous fish; since fish functional groups were harvested in this case according to their proportions of the total fish population, all functional groups that went extinct did so at the same time. (This put the threshold for local extinction of all fish functional groups combined at 4×10^{-6}.)

D Dependence of fish resilience to deforestation-induced sedimentation on local hydrological conditions

To determine how the changes brought about by deforestation depend on local conditions, we ran simulations of highland deforestation with q_b (the baseline sediment concentration in local rivers) and e (the rate at which sediment is flushed out of the system) varying within their entire ranges. Here, we took $r_X = 0.23$. Initial conditions for fish were taken to be their theoretical population maxima (i.e. 1 for each functional group); all other initial conditions were taken to be their steady-state values when no deforestation takes place and all parameters are at their baseline values. This was done in order to isolate the transient dynamics produced by different local conditions for the

same amount of deforestation pressure. In each simulation, we obtained the population of each fish functional group at $t = 20$.

We found that the effects of baseline local conditions on resilience of reef fish to deforestation-driven sedimentation was heterogeneous across functional groups. Taking the population levels of each fish functional group following 20 years of heavy deforestation on steep slopes ($r_x = 0.23$, $q_c = 0.31$) revealed the expected patterns of fish resilience being greater for higher values of e and lower values of q_b. As was the case when we examined changes in fish populations as a function of deforestation rate (Figure 2 in the main manuscript), we found that more turbid starting conditions (low e, high q_b) affected fish at higher trophic levels less than it did those at lower ones, both in absolute terms and relative to their populations in more favourable conditions (Figure D.1). Under the most turbid conditions, the herbivorous fish population was about 30 percent of what it was under the least turbid ones (Figure D.1a), and for omnivorous fish, this figure was about 25 percent (Figure D.1b). This contrasts with piscivorous fish (40 percent; see Figure D.1c) and top predators (45 percent; see Figure D.1d). This suggests that under a wide range of potential local conditions, the initial effects of deforestation-driven sedimentation are to harm fish species at lower trophic levels. We additionally found that the dependence of fish populations following deforestation on baseline river sediment concentration q_b was sigmoidal, with large changes in fish population levels around 1×10^{-2} mg cm^{-3} for most functional groups, and at somewhat greater concentrations for herbivorous fish.

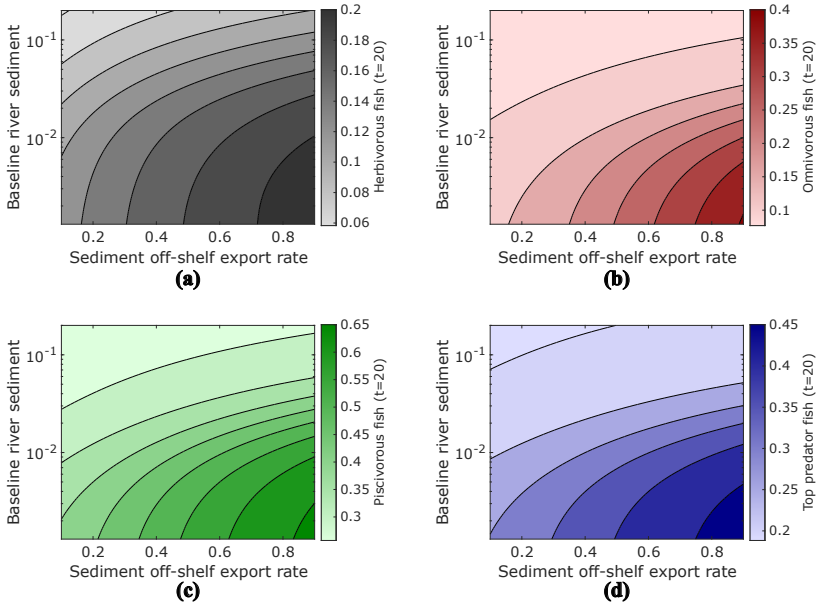

Figure D.1: Population levels of herbivorous fish (Figure D.1a), omnivorous fish (Figure D.1b), piscivorous fish (Figure D.1c), and top predator fish (Figure D.1d) after 20 years of highland logging, showing dependence on baseline sediment levels from erosion q_b and off-shelf sediment export rate e. Initial conditions for fish functional groups were taken to be that functional group's theoretical maximum population (i.e. 1) in all cases.

References

[1] C. H. R. Goatley, D. R. Bellwood, Sediment suppresses herbivory across a coral reef depth gradient, Biology Letters 8 (6) (2012) 1016–1018. doi:10.1098/rsbl.2012.0770.

[2] S. B. Tebbett, C. H. Goatley, R. P. Streit, D. R. Bellwood, Algal turf sediments limit the spatial extent of function delivery on coral reefs, Science of The Total Environment 734 (2020) 139422. doi:10.1016/j.scitotenv.2020.139422.

[3] R. Froese, D. Pauly, Fishbase, www.fishbase.org (2022).

[4] S. Tanaka, R. Nishii, A model of deforestation by human population interactions, Environmental and Ecological Statistics 4 (1) (1997) 83–92. doi:10.1023/a:1018510125512.

[5] United Nations, Department of Economic and Social Affairs, Population Division, World population prospects 2019: Online edition (2019).
URL https://population.un.org/wpp/Download/

[6] D. T. Neil, A. R. Orpin, P. V. Ridd, B. Yu, Sediment yield and impacts from river catchments to the Great Barrier Reef lagoon: a review, Marine and Freshwater Research 53 (4) (2002) 733. doi:10.1071/mf00151.

[7] A. S. Wenger, S. Atkinson, T. Santini, K. Falinski, N. Hutley, S. Albert, N. Horning, J. E. M. Watson, P. J. Mumby, S. D. Jupiter, Predicting the impact of logging activities on soil erosion and water quality in steep, forested tropical islands, Environmental Research Letters 13 (4) (2018) 044035. doi:10.1088/1748-9326/aab9eb.

[8] J. Walsh, C. Nittrouer, Contrasting styles of off-shelf sediment accumulation in New Guinea, Marine Geology 196 (3-4) (2003) 105–125. doi:10.1016/s0025-3227(03)00069-0.

[9] B. Ferré, X. D. de Madron, C. Estournel, C. Ulses, G. L. Corre, Impact of natural (waves and currents) and anthropogenic (trawl) resuspension on the export of particulate matter to the open ocean, Continental Shelf Research 28 (15) (2008) 2071–2091. doi:10.1016/j.csr.2008.02.002.

[10] T. Fung, R. M. Seymour, C. R. Johnson, Alternative stable states and phase shifts in coral reefs under anthropogenic stress, Ecology 92 (4) (2011) 967–982. doi:10.1890/10-0378.1.

[11] A. S. Hoey, D. R. Bellwood, Cross-shelf variation in the role of parrotfishes on the Great Barrier Reef, Coral Reefs 27 (1) (2007) 37–47. doi:10.1007/s00338-007-0287-x.

[12] F. X. Latrille, S. B. Tebbett, D. R. Bellwood, Quantifying sediment dynamics on an inshore coral reef: Putting algal turfs in perspective, Marine Pollution Bulletin 141 (2019) 404–415. doi:10.1016/j.marpolbul.2019.02.071.

[13] Y. Akita, T. Kurihara, M. Uehara, T. Shiwa, K. Iwai, Impacts of overfishing and sedimentation on the feeding behavior and ecological function of herbivorous fishes in coral reefs, Marine Ecology Progress Series 686 (2022) 141–157. doi:10.3354/meps13996.

[14] K. E. Havens, J. R. Beaver, D. A. Casamatta, T. L. East, R. T. James, P. Mccormick, E. J. Phlips, A. J. Rodusky, Hurricane effects on the planktonic food web of a large subtropical lake, Journal of Plankton Research 33 (7) (2011) 1081–1094. doi:10.1093/plankt/fbr002.

[15] A. L. Downing, B. L. Brown, E. M. Perrin, T. H. Keitt, M. A. Leibold, Environmental fluctuations induce scale-dependent compensation and increase stability in plankton ecosystems, Ecology 89 (11) (2008) 3204–3214. doi:10.1890/07-1652.1.

[16] Y. Tao, S. A. Campbell, F. J. Poulin, Dynamics of a diffusive nutrient-phytoplankton-zooplankton model with spatio-temporal delay, SIAM Journal on Applied Mathematics 81 (6) (2021) 2405–2432.

[17] C. M. Heggerud, H. Wang, M. A. Lewis, Transient dynamics of a stoichiometric cyanobacteria model via multiple-scale analysis, SIAM Journal on Applied Mathematics 80 (3) (2020) 1223–1246. doi:10.1137/19m1251217.

[18] J. E. Cloern, Turbidity as a control on phytoplankton biomass and productivity in estuaries, Continental Shelf Research 7 (11-12) (1987) 1367–1381. doi:10.1016/0278-4343(87)90042-2.

[19] M. M. Nugues, C. M. Roberts, Coral mortality and interaction with algae in relation to sedimentation, Coral Reefs 22 (4) (2003) 507–516. doi:10.1007/s00338-003-0338-x.

[20] D. R. Bellwood, C. J. Fulton, Sediment-mediated suppression of herbivory on coral reefs: Decreasing resilience to rising sea-levels and climate change?, Limnology and Oceanography 53 (6) (2008) 2695–2701. doi:10.4319/lo.2008.53.6.2695.

[21] A. Wakwella, P. J. Mumby, G. Roff, Sedimentation and overfishing drive changes in early succession and coral recruitment, Proceedings of the Royal Society B: Biological Sciences 287 (1941) (2020) 20202575. doi:10.1098/rspb.2020.2575.

[22] D. Souter, S. Planes, J. Wicquart, M. Logan, D. Obura, F. Staub (Eds.), Status of Coral Reefs of the World: 2020, Global Coral Reef Monitoring Network, 2020.

[23] M. O. Nadon, Stock assessment of the coral reef fishes of Hawaii, 2016. (2017). doi:10.7289/V5/TM-PIFSC-60.

[24] J. C. Blackwood, A. Hastings, P. J. Mumby, A model-based approach to determine the long-term effects of multiple interacting stressors on coral reefs, Ecological Applications 21 (7) (2011) 2722–2733. doi:10.1890/10-2195.1.

[25] V. A. Thampi, M. Anand, C. T. Bauch, Socio-ecological dynamics of Caribbean coral reef ecosystems and conservation opinion propagation, Scientific Reports 8 (1) (2018). doi:10.1038/s41598-018-20341-0.

[26] P. Dalzell, Catch rates, selectivity and yields of reef fishing, in: Reef Fisheries, Springer Netherlands, 1996, pp. 161–192. doi:10.1007/978-94-015-8779-2_7.

[27] N. Hutley, M. Boselalu, A. Wenger, A. Grinham, B. Gibbes, S. Albert, Evaluating the effect of data-richness and model complexity in the prediction of coastal sediment loading in Solomon Islands, Environmental Research Letters 15 (12) (2020) 124044. doi:10.1088/1748-9326/abc8ba.

[28] S. Albert, P. L. Fisher, B. Gibbes, A. Grinham, Corals persisting in naturally turbid waters adjacent to a pristine catchment in Solomon Islands, Marine Pollution Bulletin 94 (1-2) (2015) 299–306. doi:10.1016/j.marpolbul.2015.01.031.

[29] R. Bartley, Z. T. Bainbridge, S. E. Lewis, F. J. Kroon, S. N. Wilkinson, J. E. Brodie, D. M. Silburn, Relating sediment impacts on coral reefs to watershed sources, processes and management: A review, Science of The Total Environment 468-469 (2014) 1138–1153. doi:10.1016/j.scitotenv.2013.09.030.

[30] H. Rügner, M. Schwientek, B. Beckingham, B. Kuch, P. Grathwohl, Turbidity as a proxy for total suspended solids (TSS) and particle facilitated pollutant transport in catchments, Environmental Earth Sciences 69 (2) (2013) 373–380. doi:10.1007/s12665-013-2307-1.

[31] D. L. A. Gaveau, D. Sheil, Husnayaen, M. A. Salim, S. Arjasakusuma, M. Ancrenaz, P. Pacheco, E. Meijaard, Rapid conversions and avoided deforestation: examining four decades of industrial plantation expansion in Borneo, Scientific Reports 6 (1) (2016). doi:10.1038/srep32017.

[32] Statistics Indonesia, Penduduk Indonesia menurut provinsi 1971, 1980, 1990, 1995, 2000 dan 2010, in Indonesian (Dec. 2021).
URL https://bps.go.id/statictable/2009/02/20/1267/penduduk-indonesia-menurut-provinsi-1971-1980
html

[33] C. Vancutsem, F. Achard, J.-F. Pekel, G. Vieilledent, S. Carboni, D. Simonetti, J. Gallego, L. E. O. C. Aragão, R. Nasi, Long-term (1990–2019) monitoring of forest cover changes in the humid tropics, Science Advances 7 (10) (2021). doi:10.1126/sciadv.abe1603.

[34] T. R. McClanahan, R. Arthur, The effect of marine reserves and habitat on populations of East African coral reef fishes, Ecological Applications 11 (2) (2001) 559–569. doi:10.1890/1051-0761(2001)011[0559:teomra]2.0.co;2.